Journal of Nanobiotechnology

RESEARCH

Open Access

Metabolomics combined with physiology and transcriptomics reveal the regulation of key nitrogen metabolic pathways in alfalfa by foliar spraying with nano-selenium

Pengbo Sun[1], Gentu Ge[1], Lin Sun[2], Jian Bao[2], Muqier Zhao[1], Junfeng Hao[1], Yuhan Zhang[3], Guoshun Liu[4], Zhijun Wang[1*] and Yushan Jia[1*]

Abstract

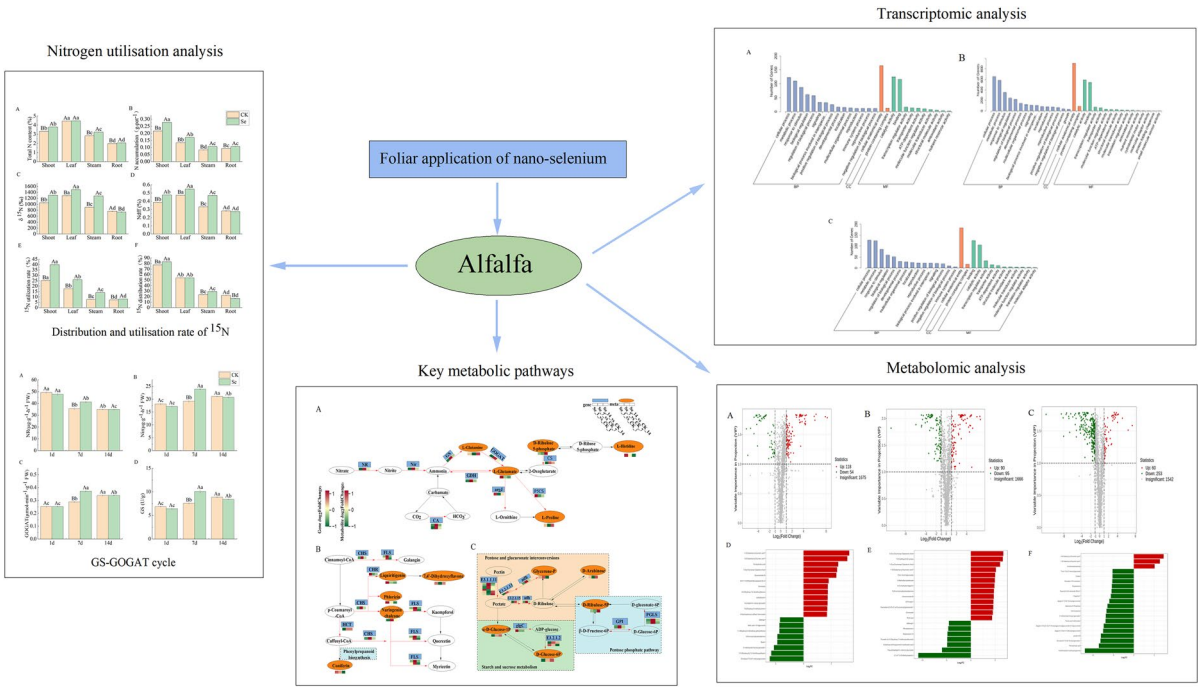
Selenium promotes plant growth and improves nutritional quality, and the role of nano-selenium in alfalfa in regulating nutritional quality is unknown. In this study, using the ^{15}N labeling method, it was found that nano-selenium could promote plant nitrogen metabolism and photosynthesis by increasing the light energy capture capacity and the activities of key enzymes of the nitrogen metabolism process, leading to an increase in alfalfa nitrogen accumulation and dry matter content. The transcriptome and metabolome revealed that nano-selenium mainly affected the pathways of 'biosynthesis of amino acids', 'starch and sucrose metabolism', 'pentose and glucuronate interconversions', 'pentose phosphate pathway', and 'flavonoid biosynthesis'. At the early stage of nano-selenium treatment, the nitrogen metabolism, sugar metabolism, and flavonoid metabolism pathways were regulated by modulating the expression of genes such as NR, Nir, GS, GOGAT, E3.1.1.11, adh, CHS, FLS, etc., which increased the amount of L-glutamic, L-histidine, glycerone-P, coniferin, naringenin chalcone, and other beneficial substances, thus promoting the acceleration of nitrogen accumulation by plants. In summary, this study provides a better understanding of the mechanisms by which nano-selenium regulates key nitrogen metabolic pathways in alfalfa.

Keywords Nano-selenium, Alfalfa, Nitrogen metabolism, Transcriptome, Metabolome

*Correspondence:
Zhijun Wang
zhijunwang321@126.com
Yushan Jia
jys_nm@sina.com
Full list of author information is available at the end of the article

© The Author(s) 2024. **Open Access** This article is licensed under a Creative Commons Attribution-NonCommercial-NoDerivatives 4.0 International License, which permits any non-commercial use, sharing, distribution and reproduction in any medium or format, as long as you give appropriate credit to the original author(s) and the source, provide a link to the Creative Commons licence, and indicate if you modified the licensed material. You do not have permission under this licence to share adapted material derived from this article or parts of it. The images or other third party material in this article are included in the article's Creative Commons licence, unless indicated otherwise in a credit line to the material. If material is not included in the article's Creative Commons licence and your intended use is not permitted by statutory regulation or exceeds the permitted use, you will need to obtain permission directly from the copyright holder. To view a copy of this licence, visit http://creativecommons.org/licenses/by-nc-nd/4.0/.

Graphical Abstract



Introduction

Selenium is an essential trace element for human and animal health; it serves as a catalytic center for selenoproteins like glutathione peroxidase, contributes to the body's antioxidant defense mechanisms, and may lower the risk of cardiovascular disease and cancer [1, 2]. As a result, inorganic selenium (selenate, selenite) was traditionally used to biofortify plants or animals in order to offer a safe supply of selenium for people [3]. However, since the range of safe doses of inorganic selenium is very small, the emergence of nanotechnology in recent years has been the key to solving this problem [4, 5]. Through physical, chemical, and biological synthesis, selenium nanoparticles with a particle size of 0–100 nm are formed, which have unique properties such as high surface activity, large specific surface area, and high catalytic efficiency [6, 7]. According to studies, nanoselenium has the following advantages over inorganic and organic selenium: high bioavailability, great stability, minimal toxicity, and high free radical scavenging ability [1, 8]. The emergence of nanomaterials such as selenium nanoparticles has become the key to the development of the next generation of precision agriculture [9].

Selenium, as a biofortifier, has a dual role similar to that of a plant hormone, promoting plant growth and metabolism at the right dose and inhibiting it beyond a threshold level [10]. A moderate amount of exogenous selenium favors photosynthesis in plants, promotes carbon and nitrogen metabolism, and increases amino acid content [11, 12]. In addition, low doses of exogenous selenium increase the content of secondary metabolites (flavonoids, phenolics, terpenes, etc.) in the plant, thus improving its nutritional quality and medicinal value of the plant [13, 14]. Nanoselenium, as a novel exogenous selenium, has a broad application throughout the agricultural neighborhood. Domokos-Szabolcsy et al. [15] found that the application of 50–100 mg L^{-1} nanoselenium made the root more extensive and dense, and the fresh weight also increased significantly; in contrast, the selenate at this concentration completely inhibited the root formation. Nano-selenium can increase the content of flavonoids, amino acids, and vitamins in cherry radish by promoting sugar metabolism and the tricarboxylic acid (TCA) cycle metabolism pathway, which improves the nutritional quality of cherry radish [16]. Compared to inorganic selenium, low-dose, low-toxicity nanoselenium has excellent dispersibility and antimicrobial capacity [17]. In addition, nanoselenium can improve the antioxidant capacity of plants by scavenging reactive oxygen species in them to adapt to adverse environments (heavy

metal pollution, drought, salinity, etc.) [18–20]. Nanoselenium also promotes the expression of lignin-related genes and an increase in metabolites (mustardiol, p-coumaryl alcohol, caffeol, and pine aldehyde) in plant roots, leading to an increase in the thickness of the cell wall to improve stress response resistance [21]. It is evident that nanoselenium is now playing an irreplaceable role in agriculture.

Alfalfa (*Medicago sativa* L.) as a high-quality forage with high protein, adaptability, and comprehensive nutritional value, is widely cultivated worldwide [22, 23]. In addition to being widely used for feeding livestock, alfalfa is rich in flavonoids, polysaccharides, sulfate derivatives, and other metabolites, which are used in edible products and have potential commercial value [24, 25]. Studies on selenium in improving alfalfa yield and nutritional quality have been reported (mostly inorganic selenium), while less research has been done on nanoselenium. Appropriate concentrations of sodium selenite increase nodule number in alfalfa roots under low nitrogen conditions and improve sugar accumulation in the plant [26]. Sodium selenite (100 mg kg^{-1}) has positive biostimulatory effects on redox metabolism, photosynthesis, and nutrition in alfalfa but is toxic at high doses [27]. Exogenous selenium will also increase the net photosynthetic efficiency of alfalfa and inhibit the formation of lignin in aboveground plants, thereby improving nutritional quality [28]. However, the molecular level mechanism of nanoselenium regulation of alfalfa nutritional quality has not yet been confirmed, especially for nitrogen regulation. Therefore, we analyzed the regulatory mechanisms of nanoselenium on nitrogen metabolism and its related metabolic pathways in alfalfa using physiological nitrogen isotope labeling, RNA-Seq sequencing, and non-targeted metabolomics (LC–MS). In this study, the physiological changes (such as photosynthetic efficiency, enzyme activity related to nitrogen metabolism, utilization, and allocation of ^{15}N) of alfalfa after nanoselenium treatment at different time periods were analyzed by the ^{15}N isotope labeling method under the optimal concentration of nanoselenium initially screened by us, and the differently expressed genes (DEGs) and differentially accumulated metabolites (DAMs) and their key pathways were identified. Our results will elucidate the molecular mechanism of nanoselenium regulation on alfalfa nitrogen metabolism and provide a theoretical framework for further application of nanoselenium.

Materials and methods

Plant cultivation and experimental conditions

The experimental soil was taken from the experimental station in Harlinger Town, Baotou City, Inner Mongolia Autonomous Region, China (longitude 110°37″–110°27″ E–40°05″–40°17″ N). The following are the original soil properties: pH, 7.4, organic matter 4.4 g kg^{-1}, total nitrogen 0.45 g kg^{-1}, fast-acting phosphorus 23.57 g kg^{-1}, fast-acting potassium 145.94 mg kg^{-1}, total selenium 0.10 mg kg^{-1}. Pot trials were conducted in a greenhouse at the Inner Mongolia Agricultural University in the Inner Mongolia Autonomous Region of China. The plant materials were the alfalfa variety 'WL232HQ'. NPs-Se was a 5% NPs-Se stock solution, provided by Shenzhen Zhigao Military and Civilian Integration Equipment Technology Research Institute. Planter size: 55 × 30 × 20 cm. 60 clover plants per pot. Stability ^{15}N isotope labeling was performed prior to foliar spraying of selenium nanoparticles. The marker used in the experiment was $K^{15}NO_3$ reagent (white crystals) with 99% abundance. Based on the content of 2 μg of ^{15}N per gram of soil in the natural state [29], 0.036 g of $K^{15}NO_3$ was applied to each pot, dissolved in 50 ml of distilled water, and injected uniformly into the soil 5 cm below the soil surface of the pots at four points with a syringe. When the alfalfa grew to about 20 cm, foliar sprays of nanoselenium at a concentration of 50 mg L^{-1} were applied at 7-day treatment intervals (sprayed three times), where sprayed distilled water was used as a control (CK). The spray rate was 1000 L hm^{-2}. Chlorophyll fluorescence parameters were determined on days 1 d, 7 d, and 14 d after the last nano- selenium treatment, while alfalfa leaves were taken to determine the enzyme activities of key enzymes of nitrogen metabolism, transcriptomes, and metabolomes for a total of three determinations, with three replications for each treatment. The treatment groups were recorded as CK_1, CK_7, CK_14, Se_1, Se_7, and Se_14. They were immediately washed with deionized water and stored on dry ice, these samples were kept at − 80 °C. The remaining plants were harvested at 14 days and divided into roots, stems, leaves, and whole plants for total N and ^{15}N determination.

Determination of plant biomass and ^{15}N indicators

The harvested alfalfa samples were dried at a constant temperature of 65°C for 48 h to determine the dry weight [22]. Dried samples were pulverized in a ball mill (MM400, Retsch, Haan, Germany), and the determination of the total nitrogen content and ^{15}N concentration ($\delta^{15}N$) was carried out using an isoprime100 stable isotope mass spectrometer and elemental analyzer (Vario Isotope Select) from Elementar, Germany. The ormulae for each indicator are given below [30]:

$$\delta^{15}\mathrm{N} = \frac{R_{sample}}{R_{standard}} - 1 \quad (1)$$

where R_{sample} is the ratio of ^{15}N to 14N in the sample, $R_{standard}$ is the ratio of ^{15}N to ^{14}N in the standard. The ^{15}N/^{14}N in the elemental nitrogen standard (air nitrogen bank) is 0.368 per cent.

^{15}N abundance in plants *Ndff*:

$$Ndff = \frac{R_{sample}}{1+R_{standard}} \times 100\% \quad (2)$$

The final ^{15}N abundance *Ndff* used for the calculation was:

$$Ndff = \frac{Ndff_{plant} - Ndff_{natural}}{Ndff_{fertiliser} - Ndff_{natural}} \times 100\% \quad (3)$$

The distribution and utilization rates for ^{15}N are calculated as follows:

$$^{15}\mathrm{N\ utilization\ rate} = \frac{Ndff \times -TotalN_{organs}}{^{15}Napplication\ rates} \times 100\% \quad (4)$$

$$^{15}\mathrm{N\ distribution\ rate} = \frac{^{15}N\ content\ of\ each\ organ}{Total^{15}N\ of\ the\ plant} \times 100\% \quad (5)$$

The cumulative amount of N is calculated as follows:

$$\mathrm{N\ accumulation} = TotalN_{organs} \times \mathrm{Dry\ matter}_{organs} \quad (6)$$

Chlorophyll fluorescence parameters

Measurements were taken between 9 and 11 a.m. Chlorophyll fluorescence parameters of the same leaves after 20 min of dark adaptation were estimated using a plant efficiency analyzer (Handy PEA, Hansatech, UK). Initial fluorescence (F_0), maximum fluorescence (F_m), variable fluorescence (F_v), maximum photochemical efficiency of PSII (F_v/F_m), and potential activity of PSII (F_v/F_0) were determined, and OJIP fluorescence curves were plotted.

Determination of key enzymes of nitrogen metabolism

Nitrate reductase (NR), nitrite reductase (Nir), glutamine synthetase (GS), and glutamate synthetase (GOGAT) were detected by using kits, which were purchased from Beijing Solarbio Science & Technology Co., Ltd. (China).

Transcriptomics analysis

Total RNA extraction, library construction, and sequencing were carried out by Wuhan Metware Biotechnology Co. Ltd. (Wuhan, China). Bioinformatics analyses were performed using the online data analysis platform Metware Cloud (https://cloud.metware.cn/). Gene expression levels were estimated as FPKM. Conditions for screening differentially expressed genes (DEGs) included |fold change| ≥ 1.5 and adjusted $p < 0.05$ [31]. Unigene sequences were aligned with KEGG and GO databases using Diamond Blastx software to complete functional gene annotation.

Metabolomics analysis

Metabolomics analysis was performed using ultra-performance liquid chromatography-mass spectrometry

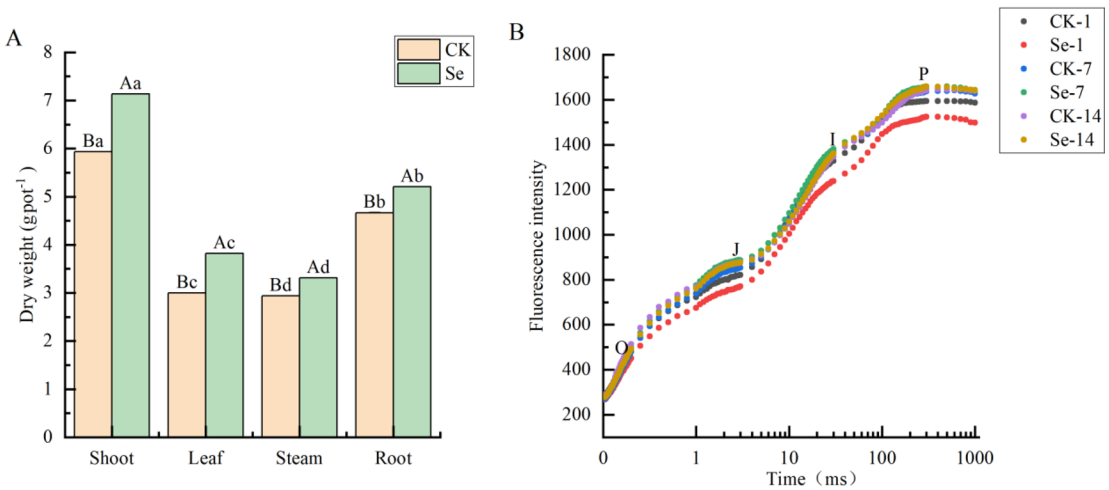


Fig. 1 Effect of nanoselenium on dry weight (**A**) and relative variable fluorescence curves (**B**) of alfalfa. CK, treatment group not sprayed with selenium; Se, treatment group sprayed with selenium. 1, 7, and 14 represent days 1, 7, and 14 after treatment, respectively. Different uppercase letters represent significant differences between selenium treatments at the same organ, and different lowercase letters represent significant differences between different organs at the same selenium treatment, $p < 0.05$. Vertical lines indicate standard errors for three replications

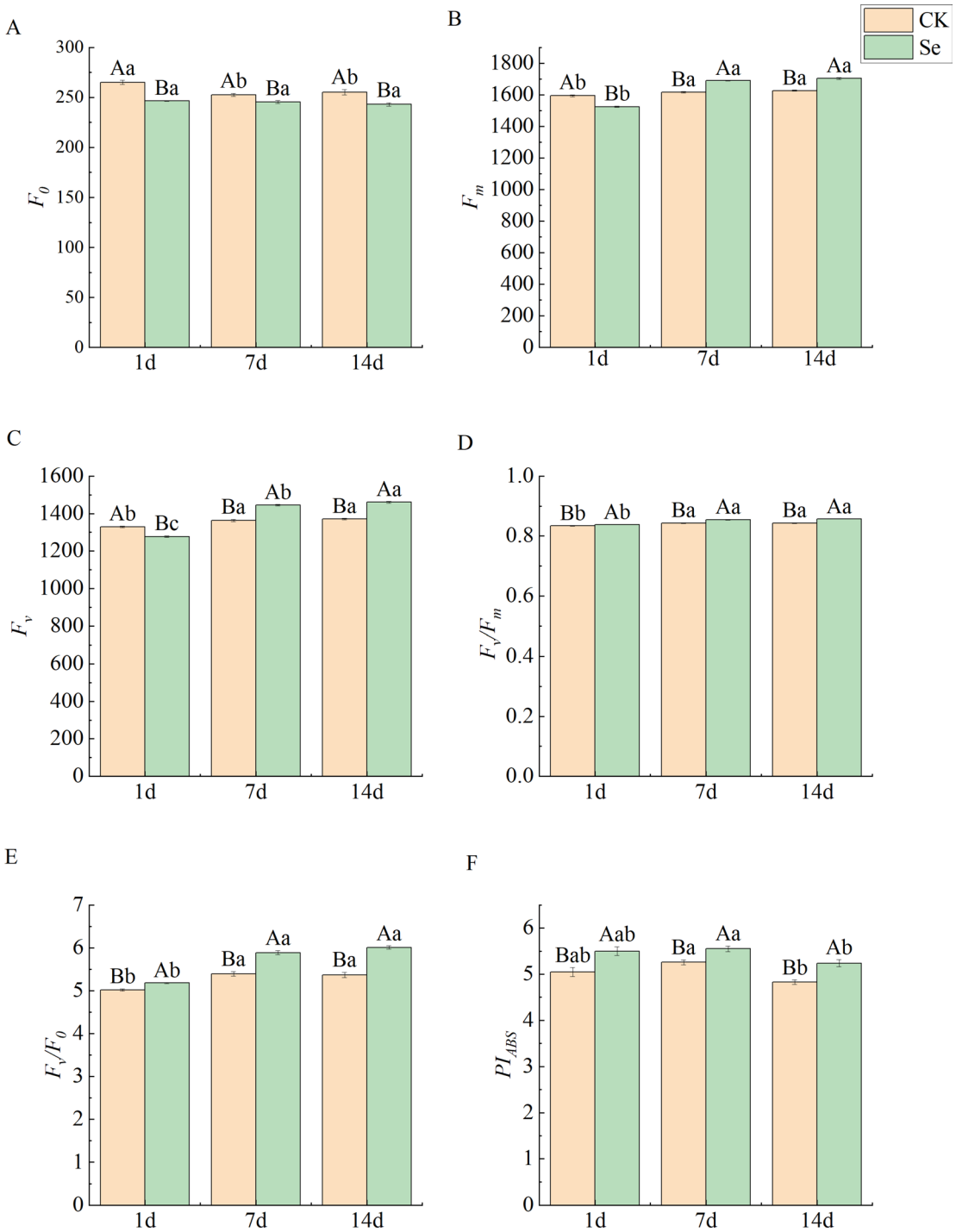


Fig. 2 Effect of nanoselenium on fluorescence parameters of alfalfa. **A** initial fluorescence (F_0); **B** maximum fluorescence (F_m); **C** variable fluorescence (F_v); **D** maximum photochemical efficiency of PSII (F_v/F_m); **E** potential activity of PSII (F_v/F_0); **F** Performance parameters based on absorbed light energy (PI_{ABS}). CK, treatment group not sprayed with selenium; Se, treatment group sprayed with selenium. 1 d, 7 d, and 14 d represent days 1, 7, and 14 after treatment, respectively. Different uppercase letters represent significant differences between selenium treatments at the same time, and different lowercase letters represent significant differences between time periods at the same selenium treatment, $p < 0.05$. Vertical lines indicate standard errors for three replications

(UPLC-MS). Firstly, the biological samples were placed in a lyophilizer (Scientz-100F) for vacuum freeze-drying and ground (30 Hz, 1.5 min) to powder form using a grinder (MM 400, Retsch). Using an electronic balance (MS105DM), 50 mg of sample powder was weighed, and 1200 μL of − 20 ℃ pre-cooled 70% methanol aqueous internal standard extract was added (less than 50 mg was added at the ratio of 1200 μL of extracting agent per 50 mg of sample). Vortex every 30 min for 30 s for a total of 6 vortexes. After centrifugation (12000 rpm, 3 min), the supernatant was aspirated, and the samples were filtered through a microporous filter membrane (0.22 μm pore size) and stored in the injection vial for UPLC-MS/MS analysis. Substance characterization based on secondary spectrum information based on self-built database MWDB (metware database). Metabolite quantification was accomplished using multiple reaction monitoring (MRM) analysis by triple quadrupole mass spectrometry.

Statistical analyses

Two-factor analysis of variance (ANOVA) was performed on the measurements of alfalfa using SAS 9.4 software (SAS Institute, Inc., Cary, NC, USA). Multiple-range tests using Duncan's were used to assess differences between treatments. Graphing with Origin version 2021 software.

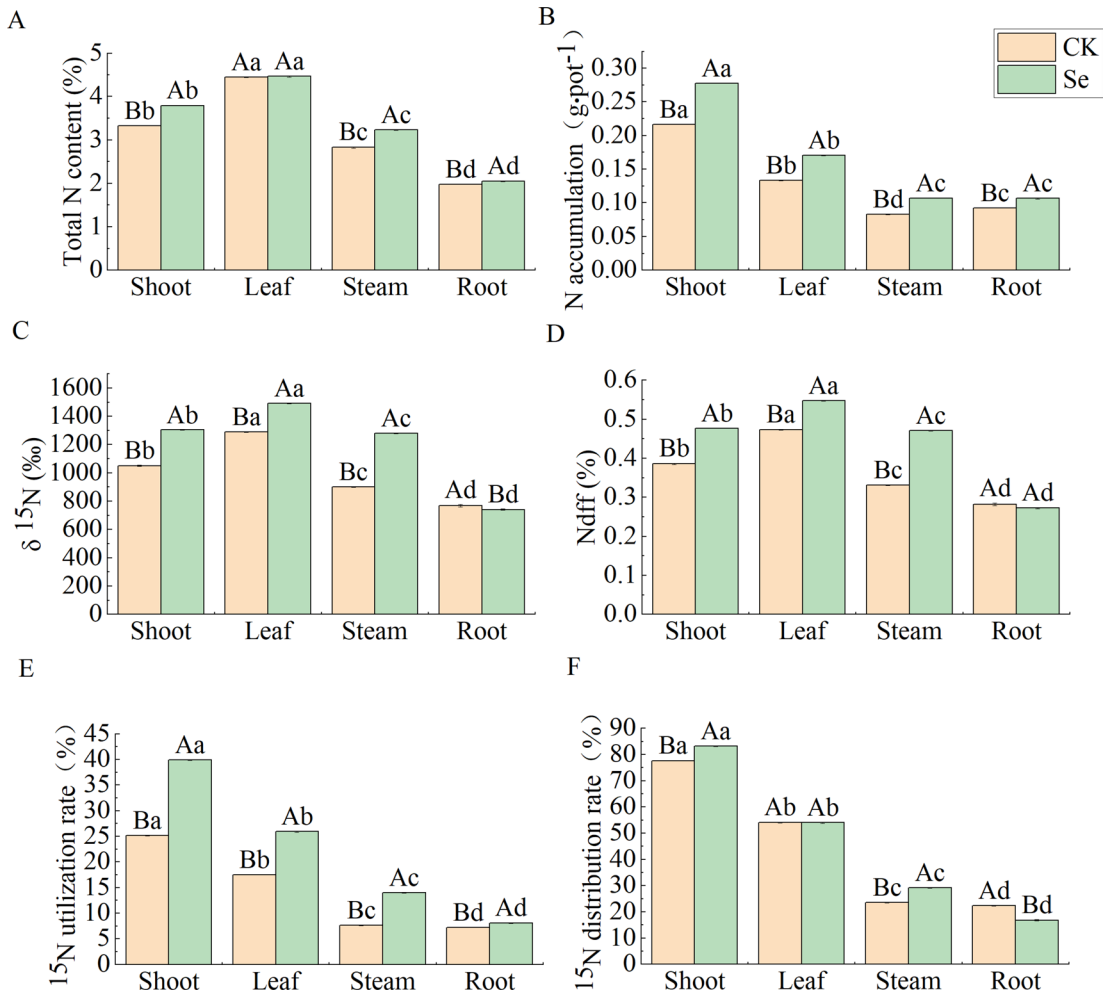


Fig. 3 Effect of nanoselenium on total nitrogen and ^{15}N partitioning in alfalfa. **A** total nitrogen content; **B** nitrogen accumulation; **C** ^{15}N concentration ($\delta^{15}N$); **D** ^{15}N abundance (*Ndff*); **E** ^{15}N utilization rate; **F** ^{15}N distribution rate. CK, treatment group not sprayed with selenium; Se, treatment group sprayed with selenium. Different uppercase letters represent significant differences between selenium treatments at the same organ, and different lowercase letters represent significant differences between different organs at the same selenium treatment, $p < 0.05$. Vertical lines indicate standard errors for three replications

Results

Plant growth and chlorophyll fluorescence parameters

The effects of nanoselenium on the dry weight of the whole plant, leaf, stem and root of alfalfa were significantly different ($p < 0.05$) (Fig. 1A). The pattern of change of dry weight of different parts of alfalfa after the two treatment groups was consistent: shoot > root > leaf > steam. The dry weight of the whole plant, leaf, stem, and root of alfalfa treated with nanoselenium was significantly higher than that of CK, which was 20.19%, 27.33%, 12.88%, and 11.59% higher than that of CK, respectively.

The OJIP curves after nanoselenium treatment had some differences at different time periods (Fig. 1B). The fluorescence intensity of the OJ, JI, and IP stages was significantly lower than that of CK at 1 d after nanoselenium treatment. This suggests that nanoselenium increased the ability of the secondary quinone receptor (QB) in PSII to accept electrons from the primary quinone receptor (QA) in PSII at an early stage. It leads to a decrease in the electron accumulation of QA in the photosynthetic electron transport chain and reduces the reduction capacity of both the fast-reducing plastoquinone (PQ) pool and the slow-reducing PQ pool. This phenomenon gradually weakened with the increase of days and was most obvious at 7 d. At this time, the fluorescence intensity of the OJ segment gradually approached that of CK, while the fluorescence intensity of the JI and IP stages was gradually higher than that of CK. At 14 d, the fluorescence intensity of the OJ segment was slightly lower than that of CK, while the fluorescence intensity of the JI and IP phases was still higher than that of CK. This suggests that nanoselenium treatment for 14 d increased the ability of the fast-reducing PQ library and the slow-reducing PQ library to be reduced, and the receptor side of the PSII reaction center was protected.

The effects of nano-selenium on chlorophyll fluorescence parameters of alfalfa leaves are shown in Fig. 2. In all three time periods, initial fluorescence (F_0) of the Se group was significantly lower than that of the CK group, and F_0 of CK showed a decreasing tendency with the increase of time, while there was no significant difference in F_0 of the Se group. With the increase of time, maximum fluorescence (F_m), variable fluorescence (F_v),

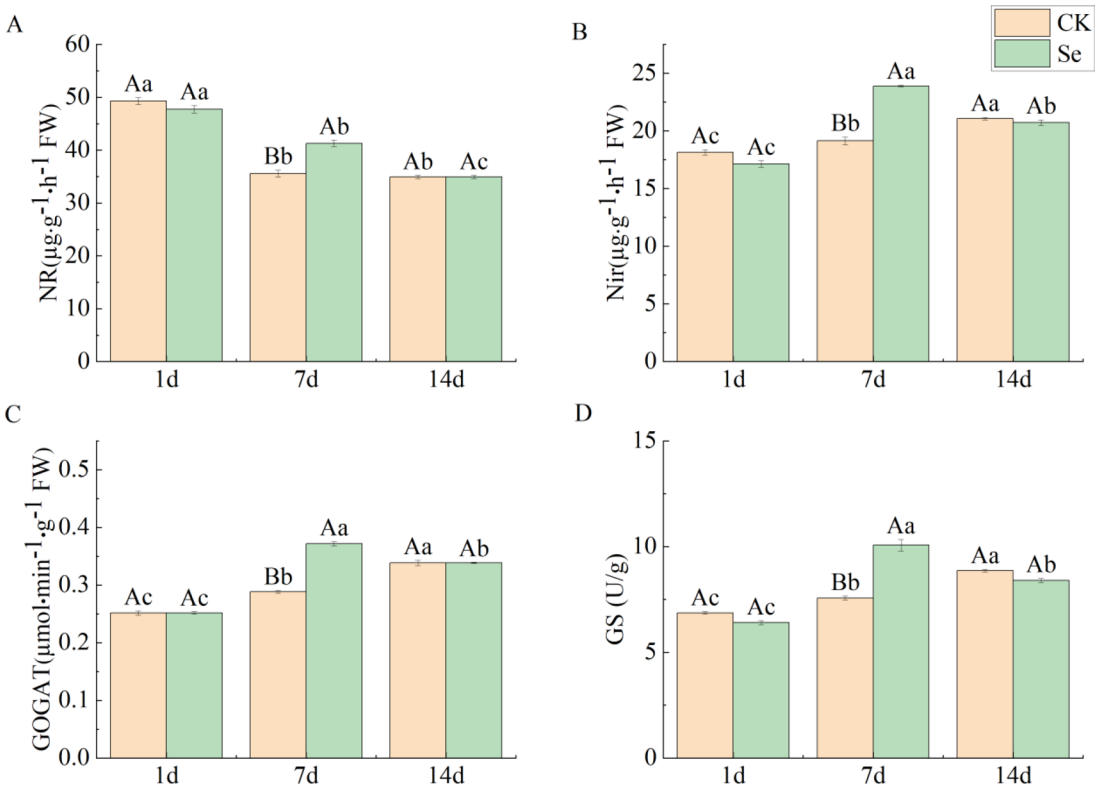


Fig. 4 Effect of nanoselenium on the activities of key enzymes of nitrogen metabolism in alfalfa leaves. **A** nitrate reductase (NR); **B** nitrite reductase (Nir); **C** glutamate synthetase (GOGAT); **D** glutamine synthetase (GS). CK, treatment group not sprayed with selenium; Se, treatment group sprayed with selenium. 1 d, 7 d, and 14 d represent days 1, 7, and 14 after treatment, respectively. Different uppercase letters represent significant differences between selenium treatments at the same time, and different lowercase letters represent significant differences between time periods at the same selenium treatment, $p < 0.05$. Vertical lines indicate standard errors for three replications

Table 1 Sequencing data statistics

Sample	Raw reads	Clean reads	Clean base(G)	Error rate (%)	Q20 (%)	Q30 (%)	GC content (%)
CK_1_1	48805208	47037012	7.06	0.02	98.4	95.01	42.05
CK_1_2	46760160	45058926	6.76	0.02	98.37	94.88	42.17
CK_1_3	49979038	48368818	7.26	0.02	98.38	94.89	42.3
CK_7_1	47196338	46010476	6.9	0.02	98.36	94.86	42.38
CK_7_2	52338658	50755050	7.61	0.02	98.38	94.89	42.3
CK_7_3	47444056	45718586	6.86	0.02	98.44	95.08	42.47
CK_14_1	46353264	45171264	6.78	0.02	98.31	94.76	42.34
CK_14_2	46591682	45221584	6.78	0.02	98.41	95.01	42.34
CK_14_3	42082560	40540476	6.08	0.02	98.25	94.65	42.51
Se_1_1	46869242	45349928	6.8	0.02	98.39	94.94	42.11
Se_1_2	49305142	47688428	7.15	0.02	98.31	94.75	42.18
Se_1_3	45361904	44097002	6.61	0.02	98.19	94.39	42.22
Se_7_1	48714020	47141790	7.07	0.02	98.46	95.16	42.48
Se_7_2	43314010	42026970	6.3	0.02	98.44	95.05	42.64
Se_7_3	48666036	47229678	7.08	0.02	98.39	94.91	42.49
Se_14_1	44293288	43036040	6.46	0.02	98.37	94.9	42.32
Se_14_2	52507874	51146462	7.67	0.02	98.51	95.18	42.51
Se_14_3	49381006	48083558	7.21	0.02	98.56	95.31	42.46

Table 2 Comparison results with the reference genome

Sample	Reads mapped	Unique mapped	Multi mapped
CK_1_1	37690171 (80.13%)	36064794 (76.67%)	1625377 (3.46%)
CK_1_2	35965181 (79.82%)	34437595 (76.43%)	1527586 (3.39%)
CK_1_3	38644793 (79.90%)	36976798 (76.45%)	1667995 (3.45%)
CK_7_1	36901262 (80.20%)	35301845 (76.73%)	1599417 (3.48%)
CK_7_2	40714836 (80.22%)	38936218 (76.71%)	1778618 (3.50%)
CK_7_3	36733743 (80.35%)	35156772 (76.90%)	1576971 (3.45%)
CK_14_1	35879291 (79.43%)	34262527 (75.85%)	1616764 (3.58%)
CK_14_2	35742751 (79.04%)	34126937 (75.47%)	1615814 (3.57%)
CK_14_3	32097388 (79.17%)	30661520 (75.63%)	1435868 (3.54%)
Se_1_1	36490646 (80.46%)	34931996 (77.03%)	1558650 (3.44%)
Se_1_2	38227559 (80.16%)	36569357 (76.68%)	1658202 (3.48%)
Se_1_3	35353567 (80.17%)	33843579 (76.75%)	1509988 (3.42%)
Se_7_1	37584466 (79.73%)	35947997 (76.26%)	1636469 (3.47%)
Se_7_2	33278834 (79.18%)	31831948 (75.74%)	1446886 (3.44%)
Se_7_3	37840765 (80.12%)	36190482 (76.63%)	1650283 (3.49%)
Se_14_1	34272966 (79.64%)	32693738 (75.97%)	1579228 (3.67%)
Se_14_2	40858404 (79.89%)	39009767 (76.27%)	1848637 (3.61%)
Se_14_3	38375447 (79.81%)	36651871 (76.23%)	1723576 (3.58%)

maximum photochemical efficiency of PSII (F_v/F_m), and potential activity of PSII (F_v/F_0) of the CK group and the Se group showed the same pattern of change, and both of them showed an upward trend. The F_m, F_v, F_v/F_m, and F_v/F_0 of the Se group were significantly higher than those of CK at 7 and 14 days. The performance parameters based on absorbed light energy (PI_{ABS}) of both CK and Se showed an increasing and then decreasing trend with the increase of time, and the PI_{ABS} of the Se group was significantly higher than that of CK at the three time periods.

Nano-selenium had a significant effect on total nitrogen content, nitrogen accumulation, $\delta^{15}N$, *Ndff*, ^{15}N utilization rate, and ^{15}N distribution rate in different parts of alfalfa ($p < 0.05$) (Fig. 3). The distribution pattern of total nitrogen content in different parts was leaf > shoot > stem > root. Compared with CK, nano-selenium significantly increased the total nitrogen content in shoot, stem, and root by 14.03%, 14.13%, and 3.54%, respectively, while the total nitrogen content in leaf was not significant. The distribution pattern of nitrogen accumulation in different parts was shoot > leaf > stem > root. Nano-selenium significantly increased the accumulation of nitrogen in shoots, leaves, stems, and roots by 28.21%, 27.81%, 28.84%, and 15.53%, respectively, compared with CK. The pattern of change of $\delta^{15}N$ and *Ndff* values in different parts was leaf > shoot > stem > root. Compared with CK, nano-selenium significantly increased $\delta^{15}N$ in shoots, leaves and stems by 24.09%, 15.65%, and 42.00%, respectively, while $\delta^{15}N$ in roots was significantly lower than that in CK by 3.59%. Nano-selenium significantly increased the *Ndff* values of shoots, leaves, and stems by 23.61%, 15.62%, and 42.39%, respectively, compared to CK, while there was no significant difference in the *Ndff* values of roots. The patterns of ^{15}N utilization rate and ^{15}N distribution rate in different parts were

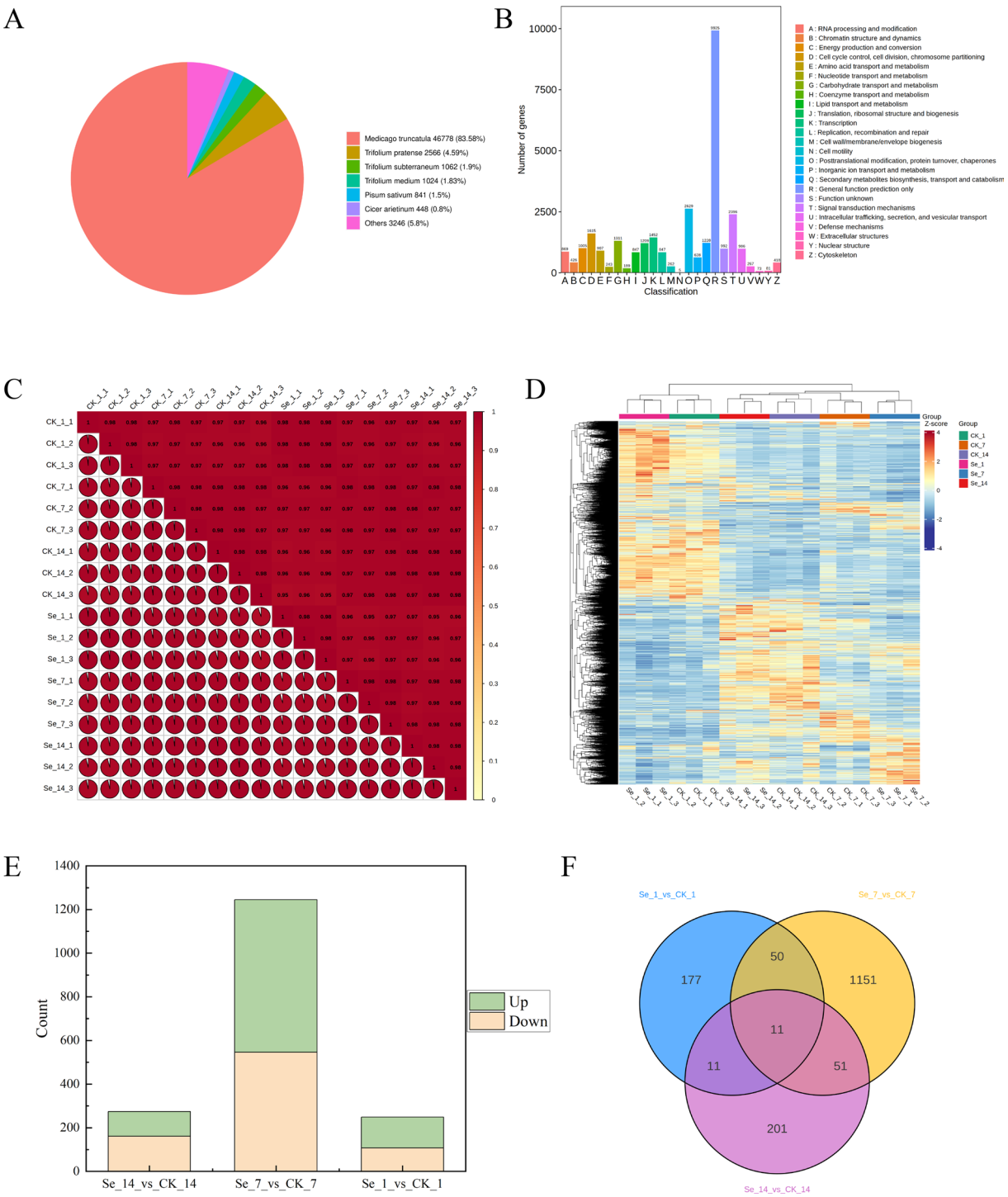


Fig. 5 Changes in DGEs expression. **A** Alfalfa unigenes information obtained by comparison in the Nr database. **B** KOG classification of the alfalfa transcriptome. **C** Correlation analysis between samples. **D** Clustering heat map of DGEs in different treatment groups. **E** The regulation of DEGs, both up and down. Up-regulation is represented by the green box, and down-regulation by the yellow box. **F** Coregulation of DEGs in all comparison groups. CK, treatment group not sprayed with selenium; Se, treatment group sprayed with selenium. CK, treatment group not sprayed with selenium; Se, treatment group sprayed with selenium. 1, 7, and 14 represent days 1, 7, and 14 after treatment, respectively

Table 3 Metabolite classification

	Number of metabolites	Percentage (%)
Alkaloids	163	8.70
Amino acids and derivatives	200	10.68
Flavonoids	319	17.03
Lignans and Coumarins	89	4.75
Lipids	185	9.88
Nucleotides and derivatives	62	3.31
Organic acids	84	4.48
Phenolic acids	184	9.82
Quinones	19	1.01
Steroids	9	0.48
Tannins	3	0.16
Terpenoids	280	14.95
Others	276	14.74
Total	1873	

shoot > leaf > stem > root. The range of ^{15}N utilization rate was 7.24% to 25.18% and 8.08% to 39.93% for CK and Se groups, respectively. Compared with CK, nano-selenium significantly increased the ^{15}N utilization rate of shoots, leaves, stems, and roots by 58.60%, 47.78%, 83.45%, and 11.57%, respectively. The nano-selenium treatment significantly increased ^{15}N distribution rate in shoot and stem by 7.09% and 23.88%, respectively, over the control. It was significantly lower than CK in roots by 24.66%, while there was no significant difference in the partition rate of ^{15}N in leaves.

Effect of nanoselenium on the activities of key enzymes of nitrogen metabolism in alfalfa leaves

Nano-selenium showed significant differences in the activities of key enzymes of nitrogen metabolism in alfalfa ($p < 0.05$) (Fig. 4). The activities of nitrite reductase (Nir), glutamate synthetase (GOGAT), and glutamine synthetase (GS) in the CK group tended to increase with time and were significantly higher than the other two time periods at 14 days. In contrast, the activities of Nir, GOGAT, and GS in the Se group showed an increasing and then decreasing trend over time, reaching a peak at 7 days, which was significantly higher than the other two time periods. The activities of nitrate reductase (NR) in both treatment groups showed a decreasing trend with

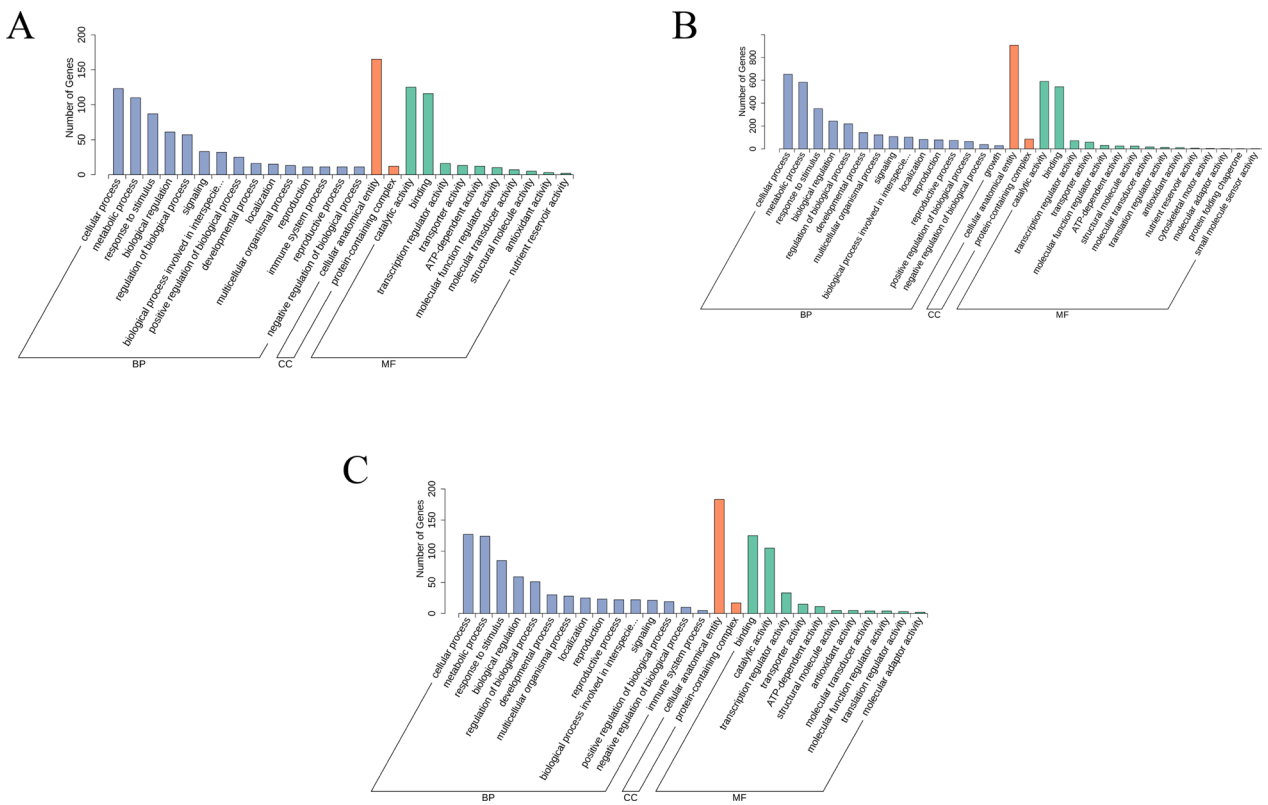


Fig. 6 Analysis of GO pathway enrichment of DEGs in different comparative treatment groups. **A** Se_1_vs_CK_1. **B** Se_7_vs_CK_7. **C** Se_14_vs_CK_14. CK, treatment group not sprayed with selenium; Se, treatment group sprayed with selenium. 1, 7, and 14 represent days 1, 7, and 14 after treatment, respectively

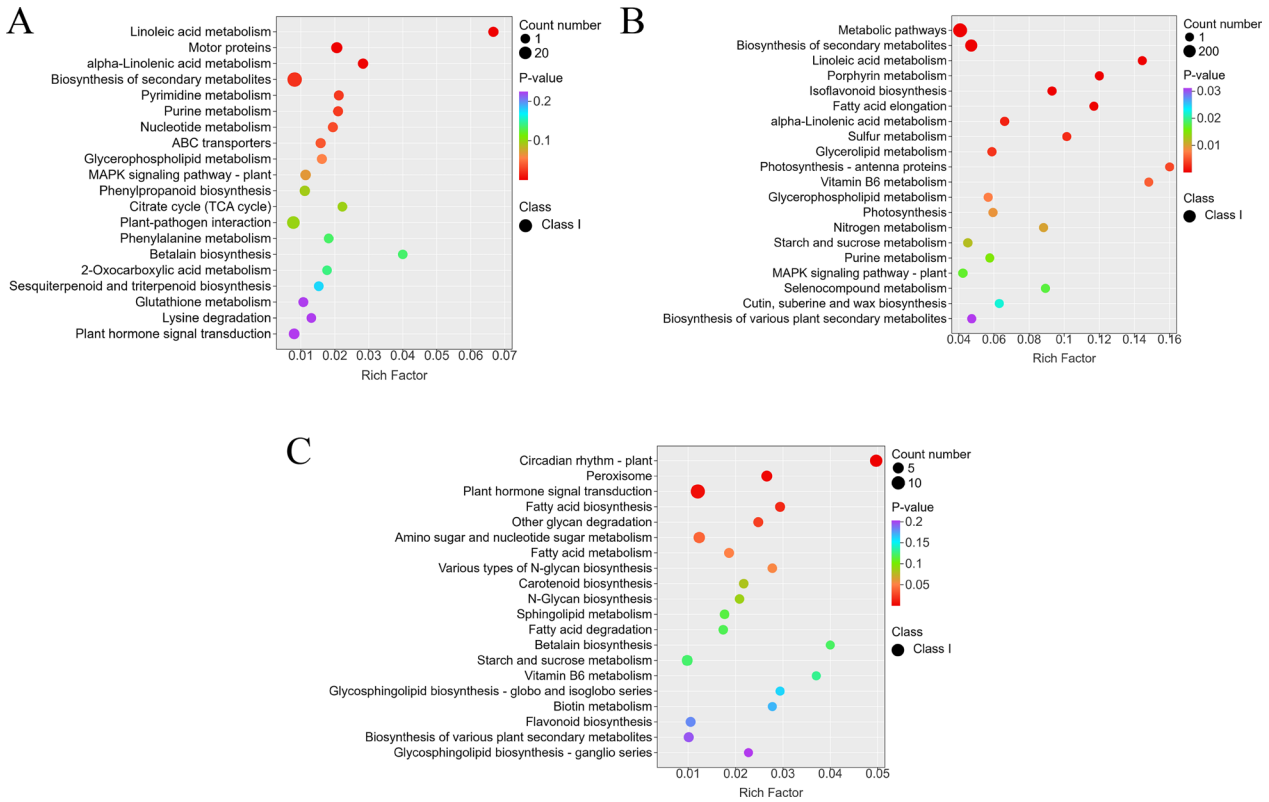


Fig. 7 Analysis of GO pathway enrichment of DEGs in different comparative treatment groups. **A** Se_1_vs_CK_1. **B** Se_7_vs_CK_7. **C** Se_14_vs_CK_14. CK, treatment group not sprayed with selenium; Se, treatment group sprayed with selenium. 1, 7, and 14 represent days 1, 7, and 14 after treatment, respectively

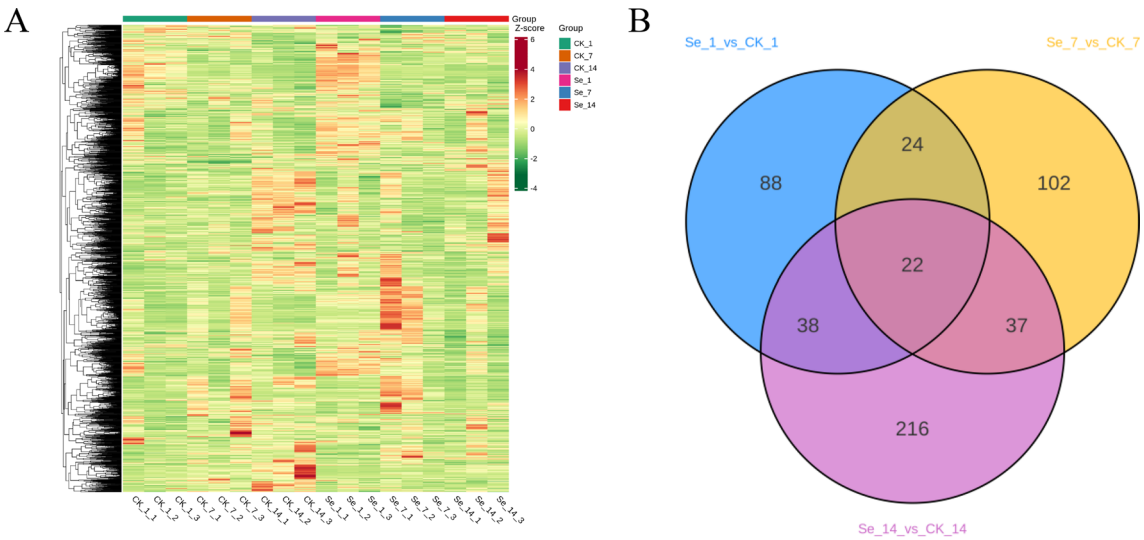


Fig. 8 Quality control of metabolomics data and changes in DAM expression. **A** Heatmap showing the results of the clustering analysis of DAMs. **B** Pairwise compare the DAMs in groups on the Venn diagram. CK, treatment group not sprayed with selenium; Se, treatment group sprayed with selenium. 1, 7, and 14 represent days 1, 7, and 14 after treatment, respectively

time and peaked at 1 day. However, the proportions of changes in the activities of various enzymes varied in different treatment groups. There was no significant difference in the activities of NR, Nir, GOGAT, and GS in the Se group at 1 and 14 days and were significantly higher than CK at 7 days (16.06%, 24.92%, 28.94%, 33.04%).

Transcriptomic analysis

Transcriptome sequencing and differentially expressed genes (DEGs) recognition

Transcriptome sequencing was performed on alfalfa leaves from three time periods after treatment (Table 1). After RNA was sequenced and quality controlled, a total of 124.44 Gb of clean base was obtained. The number of clean reads in each sample ranged from 40540476 to 51146462, and the clean base reached more than 6 Gb. The average quality of GC was 42.35%, and the average of error rate, Q20, Q30 was 0.02%, 98.38%, and 94.92%. This indicates that the sequencing quality is high and can be analyzed in the next step. The reads and uniquely mapped reads both exceeded 75% (Table 2), demonstrating the suitability of the chosen reference genome. Figure 5 shows detailed annotation information from the nonredundant (NR) and clusters of orthologous groups for eukaryotic complete genomes (KOG) databases (Fig. 5A, B). The correlation heatmap of the samples revealed that the treatment groupscorrelation coefficients were higher than 0.95 (Fig. 5C). By normalizing the data using Z-score and plotting the variance genes for each variance subgroup for hierarchical clustering heatmaps, the expression patterns of the DEGs differed significantly across treatment groups (Fig. 5D). In addition, $|\text{fold change}| \geq 1.5$ and a corrected $p < 0.05$ were used as screening conditions for pairwise comparisons to identify DEGs for the treatment groups, as shown in Fig. 5E and Table 3. A total of 274 (113 up-regulated and 161 down-regulated), 1245 (699 up-regulated and 546 down-regulated), and 249 (142 up-regulated and 107 down-regulated) DEGs were identified in the pairwise comparisons of Se_14_vs_CK_14, Se_7_vs_CK_7, and Se_1_vs_CK_1, respectively. Venn diagram analysis of the differential genes between the different comparison combinations revealed 11 common differential genes (Fig. 5F).

GO analysis and KEGG pathway analysis

Enrichment analyses were performed in the Gene Ontology (GO) and Kyoto Encyclopedia of Genes and Genomes (KEGG) databases to further evaluate the biological functions of DEGs under selenium treatment for different time periods. GO analyses classified the DEGs from the three comparison groups in the three ontologies (biological process (BP), molecular function (MF), and cellular component (CC)) (Fig. 6). Similar patterns of GO annotation distribution of DEGs in the three comparison groups. Most DEGs are assigned to 'cellular process', 'metabolic process', 'protein-containing complex', 'cellular anatomical entity', 'catalytic activity', and 'binding'. KEGG pathway enrichment was analyzed for DEGs using bubble plots, and the top 20 enriched pathways were selected (Fig. 7). Interestingly, the KEGG pathway of DEGs in Se_1_vs_CK_1 was significantly enriched in 'Glutathione metabolism' ($p < 0.05$). The KEGG pathway of DEGs in Se_7_vs_CK_7 was significantly enriched in 'nitrogen metabolism' ($p < 0.05$). The KEGG pathway of DEGs in Se_14_vs_CK_14 was significantly enriched in 'amino sugar and nucleotide sugar metabolism', 'various types of N-glycan biosynthesis' and 'N-glycan biosynthesis' ($p < 0.05$).

Metabolomic analysis

Quality control of metabolomic data

A total of 1873 metabolites were obtained from all samples. All metabolites were classified into 13 categories (Table 3). Metabolite content was normalized to construct a hierarchical clustered heat map and Venn diagram, which showed significant differences between samples (Fig. 8). We combined VIP values and fold change values ($\text{VIP} \geq 1$, $\text{fold change} \geq 2$, and $\text{fold change} \leq 0.5$) to identify the differential accurate mass search (DAMs). The distribution and expression of DAMs between the groups are shown in Fig. 9. After screening, we found 22 identical DAMs in the three comparison groups, in which the main substances were phenolic acids, flavonoids, quinones, lignans, and coumarins.

Metabolite content

There were 172 differential metabolites in Se_1_vs_CK_1 (118 up-regulated and 54 down-regulated), of which 'flavonoids', 'phenolic acids', 'terpenoids', and 'amino acids and their derivatives' accounted for 27.33%, 15.12%, 9.88%, and 7.56%, respectively. There were 185 differential metabolites (90 up-regulated and 95 down-regulated) in Se_7_vs_CK_7, of which flavonoids, phenolic acids, terpenoids, amino acids, and their derivatives accounted for 29.19%, 12.97%, 9.73%, and 7.03%, respectively. There were 313 differential metabolites (60 up-regulated and 253 down-regulated) in Se_14_vs_CK_14, of which flavonoids, phenolic acids, terpenoids, amino acids and their derivatives accounted for 27.48%, 15.02%, 11.50%, and 7.35%, respectively (Fig. 9A–C). Based on the fold change in metabolite accumulation, we identified the

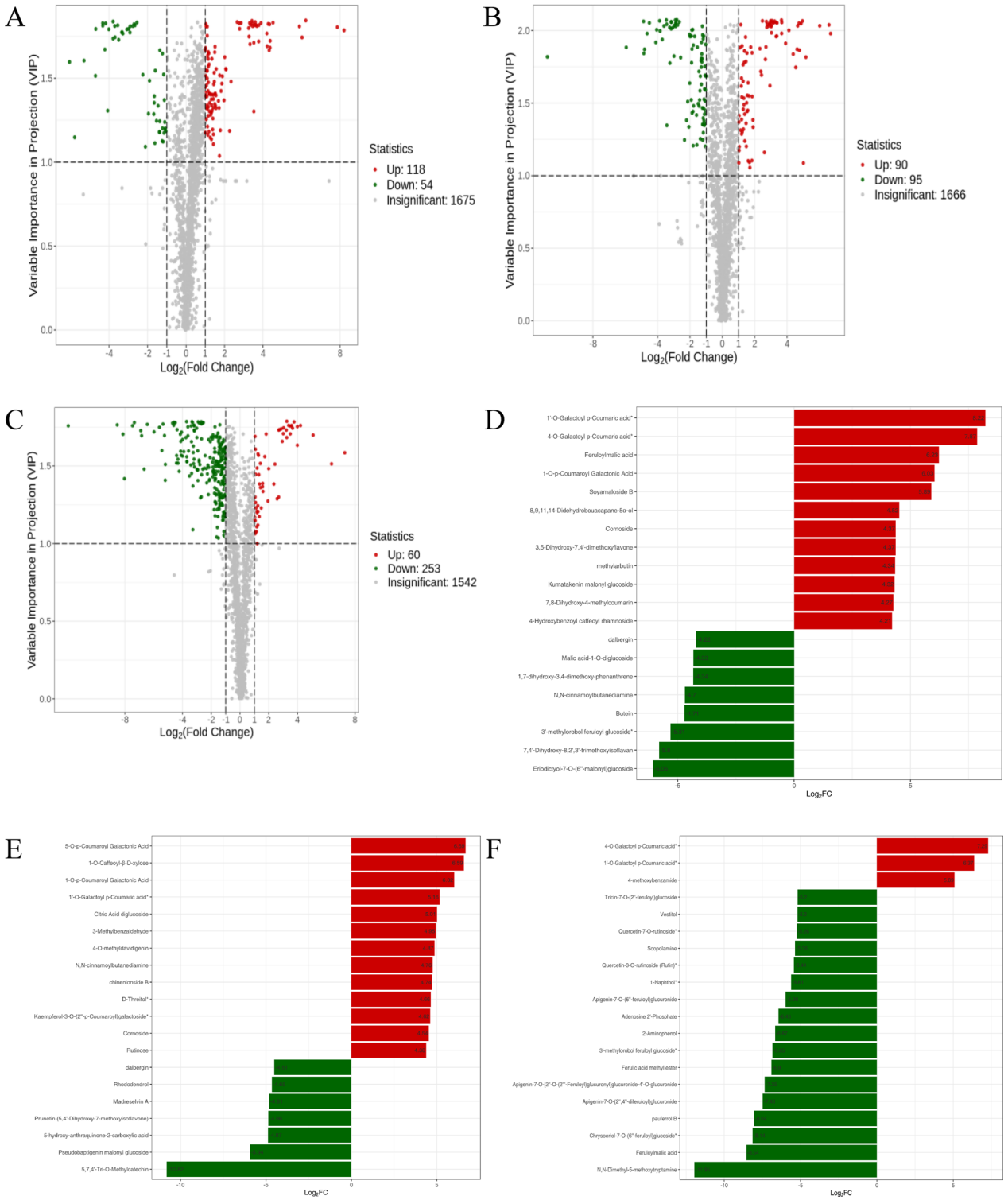


Fig. 9 DAMs up- and down-regulation in various treatment groups. **A**–**C** are volcano maps for Se_1_vs_CK_1, Se_7_vs_CK_7 and Se_14_vs_CK_14, respectively. **D**–**F** are up- and down-regulation of metabolites in the top 20 of Se_1_vs_CK_1, Se_7_vs_CK_7 and Se_14_vs_CK_14 controls, respectively. CK, treatment group not sprayed with selenium; Se, treatment group sprayed with selenium. 1, 7, and 14 represent days 1, 7, and 14 after treatment, respectively

Table 4 Differential metabolite statistics of different control groups

	Se_1_vs_CK_1		Se_7_vs_CK_7		Se_14_vs_CK_14	
	Number of metabolites	Percentage (%)	Number of metabolites	Percentage (%)	Number of metabolites	Percentage (%)
Amino acids and derivatives	13	7.56	13	7.03	23	7.35
Phenolic acids	26	15.12	24	12.97	47	15.02
Flavonoids	47	27.33	54	29.19	86	27.48
Nucleotides and derivatives	5	2.91	4	2.16	3	0.96
Quinones	5	2.91	5	2.70	8	2.56
Lignans and Coumarins	10	5.81	13	7.03	29	9.27
Tannins	1	0.58	0	0	2	0.64
Alkaloids	14	8.14	15	8.11	14	4.47
Terpenoids	17	9.88	18	9.73	36	11.50
Organic acids	4	2.33	10	5.41	18	5.75
Lipids	12	6.98	5	2.70	10	3.19
Others	18	10.47	24	12.97	37	11.82
Total	172		185		313	

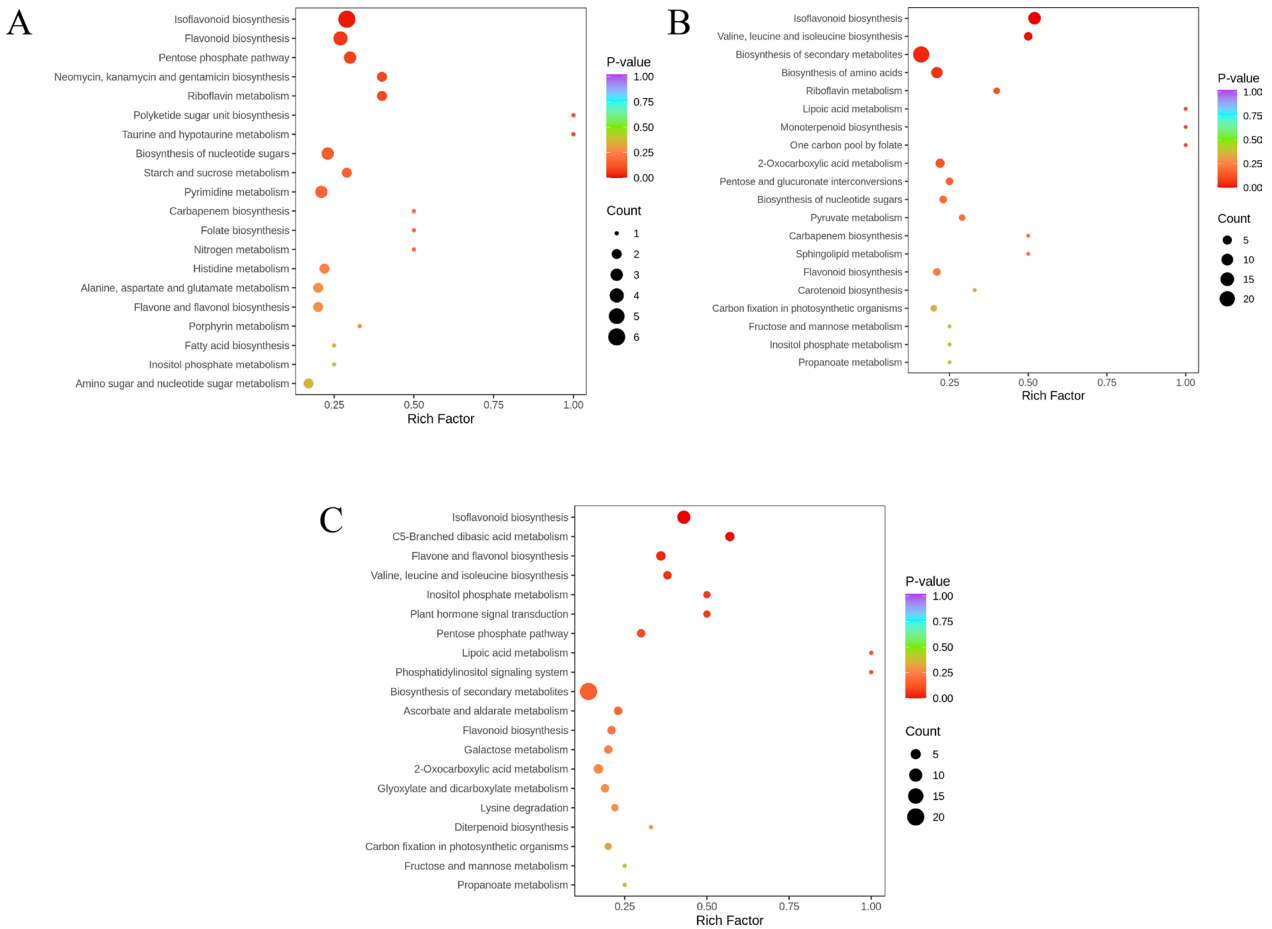


Fig. 10 KEGG up- and down-regulation is significant for the top 20 pathways. x-axis is the enrichment factor and y-axis is the pathway name. The size of the bubbles represents the number of involved. The colour of the bubbles represents the enrichment of the pathway. **A**–**C** are bubble plots of Se_1_vs_CK_1, Se_7_vs_CK_7 and Se_14_vs_CK_14, respectively. CK, treatment group not sprayed with selenium; Se, treatment group sprayed with selenium. 1, 7, and 14 represent days 1, 7, and 14 after treatment, respectively

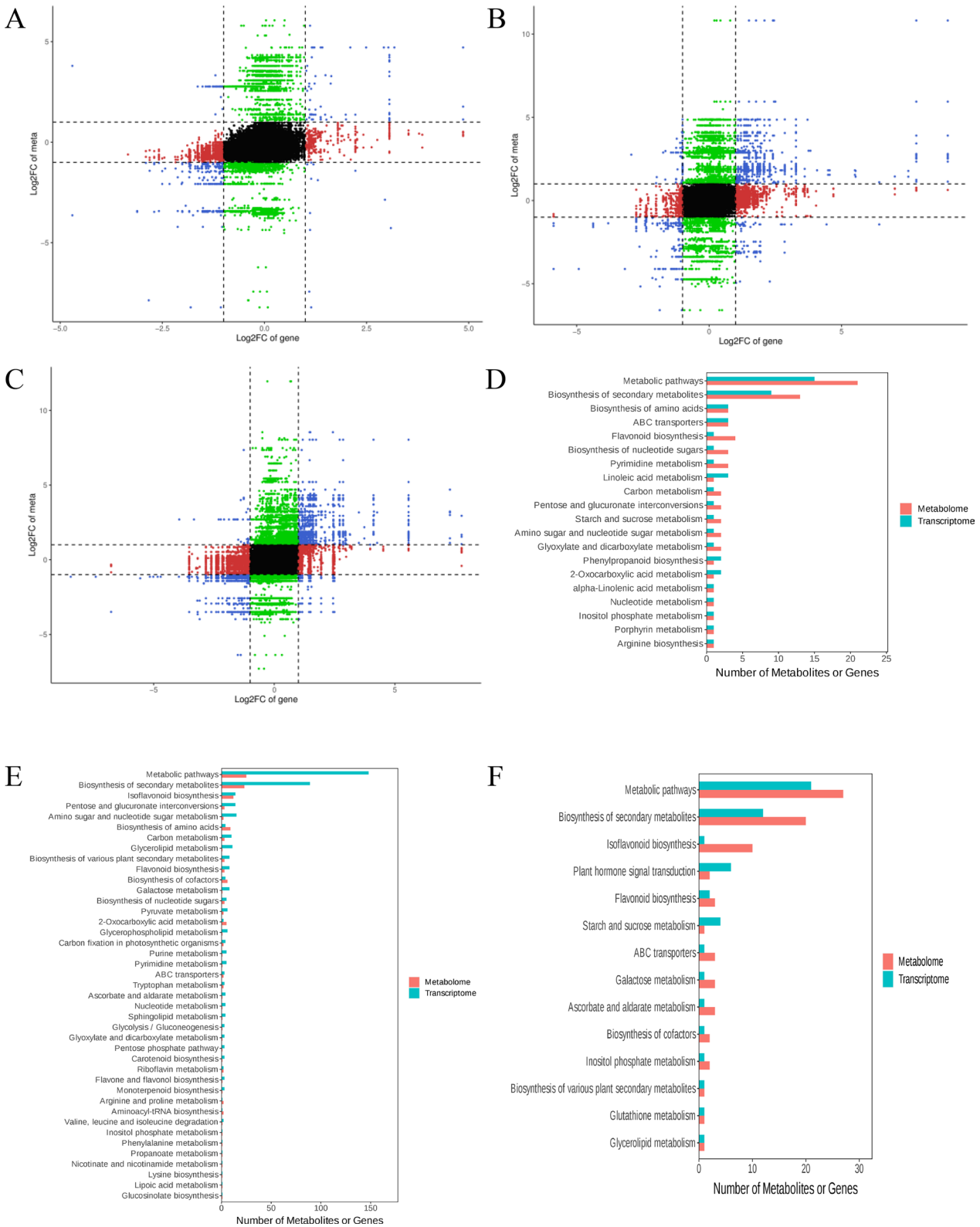


Fig. 11 Correlation analysis of transcriptomics and metabolomics data from alfalfa leaves after nanoselenium treatment. (**A**–**C**) Nine-quadrant plots showing the correlation between Se_1_vs_CK_1, Se_7_vs_CK_7, Se_14_vs_CK_14 genes and compounds. (**E**, **F**) KEGG enrichment analysis of DEGs (blue columns) and DAMs (red columns) enriched in the same pathway. CK, treatment group not sprayed with selenium; Se, treatment group sprayed with selenium. 1, 7, and 14 represent days 1, 7, and 14 after treatment, respectively

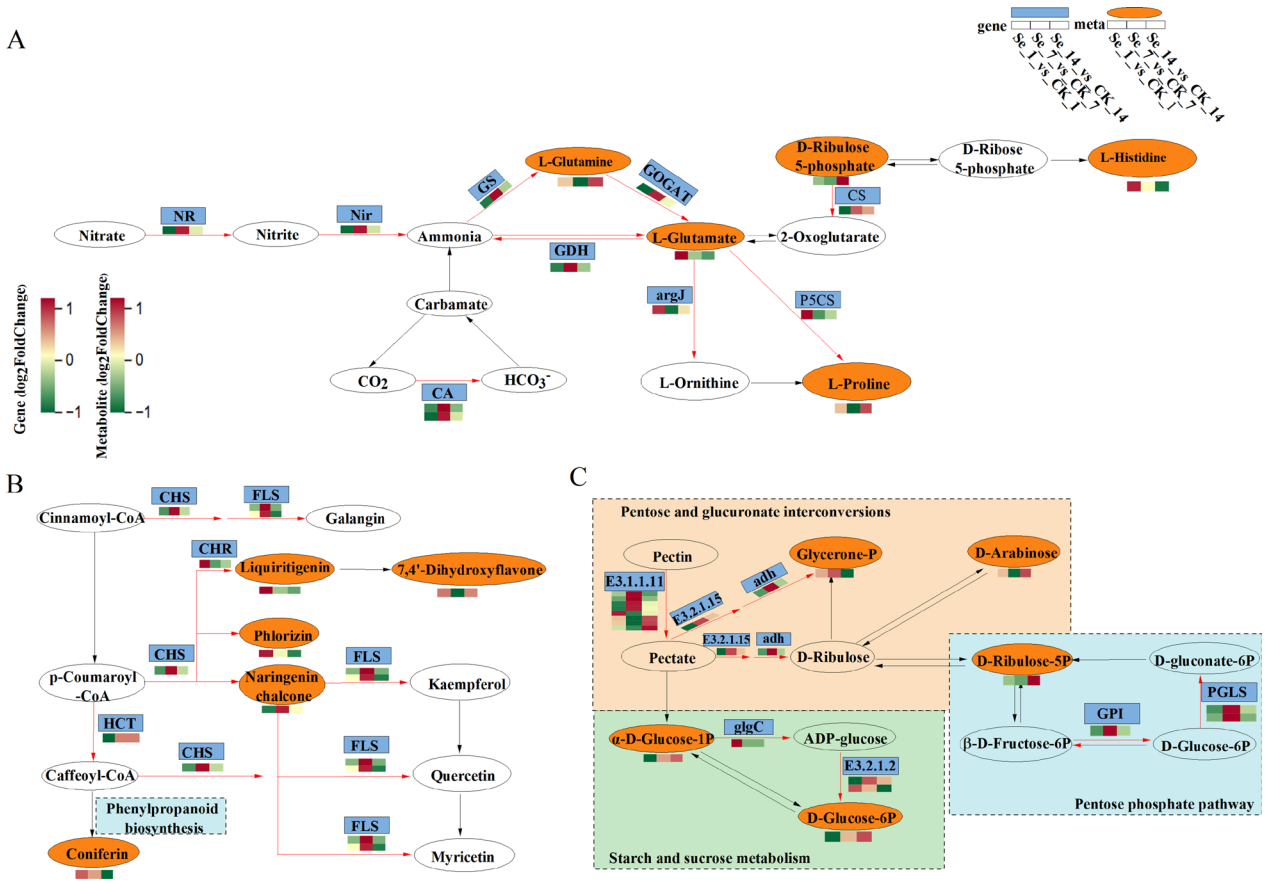


Fig. 12 Changes in major metabolic pathways in alfalfa leaves after different time periods following nanoselenium treatment. **A** The involvement of DAMs and DEGs in the amino acid biosynthesis pathway. **B** The involvement of DAMs and DEGs in the flavonoid metabolic pathways. **C** The involvement of DAMs and DEGs in the sugar metabolic pathways. Yellow ellipses represent differential metabolites with variations in content, and white ellipses represent metabolites that were not detected or whose content was not significant. Blue boxes indicate relevant enzymes affected by the differential gene. Rectangles indicate differential genes or differential metabolites, the rectangles are divided into three equal parts (Se_1_vs_CK_1, Se_7_vs_CK_7, Se_14_vs_CK_14, respectively), and the colours of the rectangles indicate the proportion of genes or metabolites regulated under nano-selenium treatment, as described in the scale bar. CK, treatment group not sprayed with selenium; Se, treatment group sprayed with selenium. 1, 7, and 14 represent days 1, 7, and 14 after treatment, respectively

top 20 DAMs with fold differences in the Se_1_vs_CK_1, Se_7_vs_CK_7, and Se_14_vs_CK_14 comparative treatment groups (Fig. 9D–F) (Table 4). Overall, changes in the content of different metabolites in alfalfa leaves were associated with selenium, suggesting that selenium modulates the content of metabolites of amino acids and their derivatives in its leaves in order to increase the total nitrogen content and alter its nutritional quality.

KEGG enrichment analysis of DAMs

We further identified key metabolic pathways involved in the response of alfalfa leaves to selenium by KEGG enrichment pathway analysis. In order to directly analyze the differences in metabolic pathways between groups, the top 20 pathways with the highest degree of enrichment in each group were selected by enrichment analysis and topology analysis (Fig. 10). The pathways 'isoflavonoid biosynthesis', 'nitrogen metabolism', 'pentose phosphate pathway', and 'polyketide sugar unit biosynthesis' were significantly enriched in the Se_1_vs_CK_1. The pathways 'isoflavonoid biosynthesis', 'valine, leucine and isoleucine biosynthesis', 'biosynthesis of amino acids', and 'riboflavin metabolism' were significantly enriched in the Se_7_vs_CK_7. The pathways 'isoflavonoid biosynthesis', 'valine, leucine and isoleucine biosynthesis', 'flavone and flavonol biosynthesis', and 'ascorbate and aldarate metabolism' were significantly enriched in the Se_14_vs_CK_14.

Joint analysis of the transcriptome and metabolome

Correlations between genes and metabolites

To investigate the relationship between DEGs and DAMs in alfalfa leaves under selenium treatment, DEGs and DAMs analyses were performed using co-expression network analysis (Pearson correlation coefficient > 0.8; $p < 0.05$). In Se_1_vs_CK_1, Se_7_vs_CK_7, and Se_14_vs_CK_14, correlation analyses showed that many of the genes were highly positively correlated with metabolites (Fig. 11A–C). These findings suggest that the genes involved may directly or indirectly control changes in the accumulation of these metabolites. KEGG enrichment analysis showed that comparisons of Se_1_vs_CK_1, Se_7_vs_CK_7, and Se_14_vs_CK_14 revealed 20, 41 and 14 pathways, respectively (Fig. 11D–F).

Critical pathway analysis

Combining transcriptome and metabolome analyses, we found that the differential genes and metabolites were mainly enriched in the pathways 'biosynthesis of amino acids', 'starch and sucrose metabolism', 'flavonoid biosynthesis', 'pentose and glucuronate interconversions', and 'pentose phosphate pathway' in five pathways (Fig. 12). Some of the key genes and enzymes in these enriched pathways, such as nitrate reductase (NR), nitrite reductase (Nir), glutamate dehydrogenase (GDH), carbonic anhydrase (CA), glutamine synthetase (GS), glutamate synthase (GOGAT), delta-1-pyrroline-5-carboxylate synthetase (P5CS), chalcone synthase (CHS), chalcone reductase (CHR), and alcohol dehydrogenase (adh) were significantly up-regulated and down-regulated. These up-regulated and down-regulated genes and enzymes lead to further changes in the expression levels of metabolites, including amino acids (L-glutamate, L-histidine, L-proline), flavonoids (liquiritigenin, 7,4'-dihydroxyflavone, phlorizin), sugars (α-D-glucose-1P, ribulose-5P, D-arabinose, D-glucose-6P) and other metabolites (coniferin, Glycerone-P). By improving antioxidant, sugar metabolism, and nitrogen metabolism, ultimately leading to increased biomass and nitrogen levels in alfalfa.

Discussion

Forage yield is one of the most important economic indicators of the size of forage productivity and is the most intuitive expression of plant net photosynthesis [32, 33]. Appropriate doses of exogenous selenium can significantly increase plant biomass [34, 35]. This was also the case in our study, where foliar spraying of nanoselenium significantly increased the dry weight of alfalfa roots, stems, and leaves (Fig. 1A). This is due to the fact that moderate amounts of selenium increase the light energy capture capacity and conversion efficiency of the plant, thus increasing photosynthesis [36, 37]. In our study, nanoselenium maximized the reduction of PQ pools and PI_{ABS}, thereby enhancing electron transfer, which was further elucidated by chlorophyll fluorescence parameters (Fig. 1B). Transcriptomic and metabolomic data indicated that the Se_7 treatment group up-regulated the expression of light-harvesting chlorophyll-protein complex-related genes in alfalfa leaves, including *MsG0380017141.01*, *MsG0680030760.01*, *MsG0680030757.01*, and *MsG0680030758.01*, thereby enhancing the metabolic pathway of Photosynthesis—antenna proteins (Fig. 7B). The enhancement of the metabolic pathway of photosynthesis-antenna proteins implies that the plant body is more efficient for the conversion of light energy and improves the ability to fix carbon [27, 38]. And the Se_7 treatment group finally led to the accumulation of 10-formyl-THF, glycerone-P, D-threitol, meso-erythritol, and other substances. This phenomenon diminished at 1d and 14d. This suggests that at an early stage nanoselenium can maximize photosynthesis in plants and thus increase biomass. This may be due to the fact that at 1 d, nanoselenium has just entered the chloroplast to participate in selenium metabolism, resulting in some metabolic disturbances [39, 40]. And at 14 d, as the conversion of selenium from nano-selenium to selenium-containing proteins or small molecule selenium-containing derivatives in the chloroplasts is completed, and as the newborn parts of the plant grow, the selenium-containing proteins are redistributed from the old leaves to the newborn parts of the roots and leaves, the degree of stimulation of the chloroplasts becomes less [41–43]. Therefore, it is possible that during the prenatal period (1–7 d), selenium is metabolically converted to stimulate the chloroplasts to respond by enhancing the photosynthesis-antenna protein pathway, thereby enhancing photosynthesis and providing energy for the plant's strenuous activities.

Nitrogen is one of the most demanded mineral elements in plant growth and is involved in the synthesis of organic compounds such as proteins, nucleic acids, chlorophyll, enzymes, vitamins, and alkaloids [44, 45]. Nitrogen is an important nutrient necessary for plant growth and development and plays an important role in promoting plant growth, organ formation, flower bud differentiation, and improving yield and quality [46, 47]. ^{15}N isotope labeling is an important research method to investigate nitrogen use and redistribution in plants [48, 49]. In our study, using ^{15}N-labelled tracer method, it was clarified that nanoselenium can improve the use of nitrogen in alfalfa and promote the redistribution of ^{15}N to different parts of alfalfa, which ultimately leads to an increase in the accumulation of nitrogen in roots, stems,

and leaves. Nitrate reductase (NR) exists widely in plants and microorganisms and is a key rate-limiting enzyme in the nitrogen assimilation process of higher plants. Its activity level directly reflects the strength of plants' ability to reduce nitrate nitrogen to nitrite and is closely related to the ability of plants to absorb and accumulate nitrogen [50, 51]. Nitrite reductase (Nir) can further reduce nitrite to NH_4^+ and participate in the subsequent metabolism of amino acids [52]. In our study, the Se_7 treatment group could significantly enhance the activities of NR and Nir in alfalfa leaves (Fig. 4). From the transcriptome data, it was found that the Se_7 treatment group significantly up-regulated the expression of genes related to the control of NR (*MsG0580027470.01*) and Nir (*MsG0380016934.01*), which enhanced the nitrogen metabolic pathway (Figs. 7B, 12A). It further demonstrated that nanoselenium could control the enhancement of nitrogen metabolism-related enzyme activities by regulating the up-regulation of their genes, leading to the efficient use of nitrogen in plants. In addition, NR is gradually decreasing with time, while the activities of Nir, GS, and GOGAT are increasing. The reason for this is that plants begin to be in the late stage of the nutrient growth period and gradually shift to the reproductive growth period. NR, as the first restriction enzyme, will respond to this change, and its activity begins to decline, weakening the uptake of nitrate [53]. In the early stage, when NR activity is stronger, it accumulates a large amount of nitrite. This accumulation leads to an increase in the activity of Nir, GS, GOGAT, and other related enzymes in the subsequent nitrogen metabolism process, which accelerates the conversion of nitrite into the amino acids and proteins required by the plant. The activity of NR declined earlier than that of Nir, and the results of this study are consistent with the study by Feller et al.[54]. The GS-GOGAT pathway regulates nitrogen assimilation, particularly GS, which is a key enzyme for ammonia assimilation. The products of this pathway serve as signals or precursors, further regulating primary and secondary plant metabolism. In our study, it was found from transcriptomic and metabolomic data that L-glutamic, L-proline, L-histidine, L-α-glutamyl-L-glutamic, N-acetyl-DL-phenylalanine, and other amino acid derivatives due to the expression of the relevant genes at different time intervals led to their up-regulated and down-regulated to varying degrees (Figs. 10, 12A). Among them, the Se-7 treatment group could significantly enhance the activities of GS and GOGAT in alfalfa leaves (Fig. 4), and the Se-7 treatment group significantly up-regulated the expression of genes related to the control of GS (*MsG0280007136.01*) and GOGAT (*MsG0780040437.01*), which enhanced the amino acid biosynthesis pathway (Figs. 7B, 12A). The conclusions of this study are consistent with the study by Li et al. [55]. Thus, nano-selenium partially facilitates the early formation of amino acids, which are involved in subsequent pathways such as amino acid, carbohydrate, and secondary metabolism [56].

Throughout nitrogen metabolism, the enhanced metabolic activity also means that more energy is required to support it. Glycolysis and the pentose phosphate pathway provide the precursors for the biosynthesis of amino acids as well as the energy required for the activity [57]. Here, nanoselenium altered the 'starch and sucrose metabolism', 'pentose and glucuronate interconversions', and 'pentose phosphate pathway'. The expression of E3.1.1.11 was first altered to regulate glucose metabolism through a series of biochemical reactions, including α-D-glucose-1P, D-glucose-6P, ribulose-5P, glycerone-P, D-arabinose, and other metabolites (Fig. 12C). Among them, D-glucose-6P is a key node connecting photosynthesis and respiration and is involved in the production of ATP and NADPH, while α-D-glucose-1P is a precursor of starch synthesis and sucrose transport and is able to produce starch and achieve intercellular sucrose transport [58, 59]. In our study, the metabolites of α-D-glucose-1P, D-glucose-6P, and ribulose-5P after nanoselenium treatment were progressively up-regulated with time compared to CK, whereas the other amino acids and their derivatives, such as L-histidine and L-glutamic, showed the opposite trend (Fig. 12A, C). This further suggests that the pre-treatment with nanoselenium may consume a large amount of D-Glucose-6P to produce ATP and NADPH, which are further involved in the biosynthesis of amino acids [60, 61]. Tang et al. [62] and Liu et al. [63] also showed that selenium can regulate sugar metabolism in plants, thereby affecting amino acid biosynthesis. In contrast, the regulation of sugar and nitrogen metabolism by nanoselenium was bidirectional, with positive effects on both, thus leading to an increase in the final nitrogen content and dry matter content of alfalfa.

Flavonoids are a class of plant secondary metabolites synthesized via the phenylpropane pathway, and more than 9,000 different compounds have been identified to date that are important for plant growth and development [64]. Flavonoid compounds have been identified as plant signals and developmental regulators of legume nodulation and have long been known to play a key role in actinomycete root nodulation processes [65]. Exogenous selenium can regulate the accumulation of plant flavonoids by affecting the expression of relevant structural and regulatory genes [66, 67]. We found that nano-selenium can inhibit gene expression of enzymes controlling CHS (*MsG0780040080.01*), FLS (*MsG0580027458.01*, *MsG0580027459.01*), and other related enzymes in the early stage, thus inhibiting other metabolic pathways and thereby increasing coniferin,

phlorizin, liquiritigenin, and other flavonoid compounds. However, in the middle stage, it can promote the gene expression of enzymes related to the control of CHS, FLS, etc. and enhance flavonoid compounds such as naringenin chalcone (Fig. 12B). Coniferin, as a precursor for lignin and lignin biosynthesis, helps plants to better absorb essential nutrients (e.g., nitrogen, phosphorus, potassium) and also facilitates resistance to invasive pathogens, thus promoting plant growth and development [68]. Naringenin chalcone, an intermediate in the synthesis pathway of flavonoids, is cyclized to naringenin in a series of reactions that catalyze the first biochemical reaction in flavonoid production [69]. In turn, naringenin can participate in free radical coupling reactions and be doped into lignin polymers, and it has an important role in regulating nitrogen fixation in plants [70]. Knockdown of chalcone synthase expression was found to reduce the levels of specific flavonoids, resulting in severely impaired nodulation, whereas by supplementing the plants with naringenin, an upstream intermediate in flavonoid biosynthesis, the formation of rhizomes could be promoted and the nitrogen-fixing efficiency of the plants could be improved [65]. At the same time, naringenin incorporated into lignin polymers reduces the lignin content of the plant and favors the enhancement of plant stem availability, thus improving the nutritional quality of the plant [71]. Thus, nano-selenium can augment flavonoid compounds in plants, improving plant resilience while also stimulating nitrogen fixation efficiency, resulting in increased nitrogen levels in plants.

Conclusion

In this study, we investigated the response mechanisms of key metabolic pathways, including nitrogen metabolism in alfalfa under nano-selenium treatment using multi-omics analysis and ^{15}N labeling. Nano-selenium promoted plant nitrogen metabolism and photosynthesis by increasing the light energy capture capacity and the activities of key enzymes of the nitrogen metabolism process (NR, Nir, GS, and GOGAT), leading to an increase in alfalfa nitrogen accumulation and dry matter content. Moreover, the transcriptome and metabolome revealed that nanoselenium mainly affected the pathways of 'biosynthesis of amino acids', 'starch and sucrose metabolism', 'pentose and glucuronate interconversions', 'pentose phosphate pathway', and 'flavonoid biosynthesis'. At the initial stage of nanoselenium treatment, the 'nitrogen metabolism', 'sugar metabolism', and 'flavonoid metabolism pathways' were regulated by modulating the expression of genes such as NR, Nir, GS, GOGAT, E3.1.1.11, adh, CHS, and FLS. It increases the content of beneficial substances such as L-glutamic, L-histidine, glycerone-P, coniferin, naringenin chalcone, etc., thus promoting the acceleration of nitrogen accumulation in plants. And this effect gradually diminishes in the later stages. The results of this study are expected to provide new insights into the molecular pathways of alfalfa in response to nano-selenium supply at different times and provide a theoretical basis for the safe and efficient production of selenium-enriched alfalfa.

Acknowledgements
This work was supported by a grant from the National Technical System of Forage Industry for Dry Grass Storage (CARS-34-25), the development and demonstration of key technologies for high quality forage production and grass product processing (CCPTZX2023B07). Thank to Wuhan Metware Biotechnology (Wuhan, China) for its constructive comments and technical support with microbiological data analysis in this manuscript.

Author contributions
Conceptualization, methodology, data curation, writing—original draft preparation and writing—review and editing: PS. Methodology: JB, MZ, JH, GL, and YZ. Writing—original draft preparation, writing—review and editing, investigation and resources: LS. Writing—review and editing: GG. Project administration and funding acquisition: YJ, ZW. All authors have read and agreed to the published version of the manuscript.

Availability of data and materials
All data generated or analyzed during this study are included in this published article within each editable graph.

Declarations

Ethics approval and consent to participate
Not applicable.

Consent for publication
Not applicable.

Competing interests
The authors declare no competing interests.

Author details
[1]Key Laboratory of Forage Cultivation, Processing and High Efficient Utilization, Ministry of Agriculture, People's Republic of China, Key Laboratory of Grassland Resources, Ministry of Education, People's Republic of China, College of Grassland, Resources and Environment, Inner Mongolia Agricultural University, Hohhot, China. [2]Inner Mongolia Academy of Agricultural and Animal Husbandry Sciences, Hohhot, China. [3]Forestry and Grassland Work Station of Inner Mongolia, Hohhot, China. [4]Forestry Station of Xining, Xining, Qinhai, China.

Received: 3 August 2024 Accepted: 11 December 2024
Published online: 05 January 2025

References

1. Shi M, Zhang T, Fang Y, Pan C, Fu H, Gao S, Wang J. Nano-selenium enhances sugarcane resistance to *Xanthomonas albilineans* infection and improvement of juice quality. Ecotoxicol Environ Saf. 2023;254:114759. https://doi.org/10.1016/j.ecoenv.2023.114759.
2. Li B, Liu X, Yu T, Lin K, Ma X, Li C, Yang Z, Tang Q, Zheng G, Qin J. Environmental selenium and human longevity: an ecogeochemical perspective. Chemosphere. 2024;347:140691. https://doi.org/10.1016/j.lwt.2015.03.046.
3. Hall JA, Van Saun RJ, Nichols T, Mosher W, Pirelli G. Comparison of selenium status in sheep after short-term exposure to

high-selenium-fertilized forage or mineral supplement. Small Ruminant Res. 2009;82(1):40–5. https://doi.org/10.1016/j.smallrumres.2009.01.010.
4. Zhang B, Zhou K, Zhang J, Chen Q, Liu G, Shang N, Qin W, Li P, Lin F. Accumulation and species distribution of selenium in Se-enriched bacterial cells of the Bifidobacterium animalis 01. Food Chem. 2009;115(2):727–34. https://doi.org/10.1016/j.foodchem.2008.12.006.
5. Sun P, Ge G, Sun L, Du S, Liu Y, Yan X, Zhang J, Zhang Y, Wang Z, Jia Y. Effects of selenium enrichment on fermentation characteristics, selenium content and microbial community of alfalfa silage. BMC Plant Biol. 2024;24(1):555. https://doi.org/10.1186/s12870-024-05268-1.
6. Gao X, Matsui H. Peptide-based nanotubes and their applications in bionanotechnology. Adv Mater. 2005;17(17):2037–50. https://doi.org/10.1002/adma.200401849.
7. Ferrari L, Cattaneo DM, Abbate R, Manoni M, Ottoboni M, Luciano A, von Holst C, Pinotti L. Advances in selenium supplementation: from selenium-enriched yeast to potential selenium-enriched insects, and selenium nanoparticles. Anim Nutr. 2023;14:193–203. https://doi.org/10.1016/j.aninu.2023.05.002.
8. García Márquez V, Morelos Moreno Á, Benavides Mendoza A, Medrano MJ. Ionic selenium and nanoselenium as biofortifiers and stimulators of plant metabolism. Agron. 2020;10(9):1399. https://doi.org/10.3390/agronomy10091399.
9. Buriak JM, Liz-Marzán LM, Parak WJ, Chen X. Nano and plants. ACS Nano. 2022;16(2):1681–4. https://doi.org/10.1021/acsnano.2c01131.
10. Zhu Z, Chen Y, Shi G, Zhang X. Selenium delays tomato fruit ripening by inhibiting ethylene biosynthesis and enhancing the antioxidant defense system. Food Chem. 2017;219:179–84. https://doi.org/10.1016/j.foodchem.2016.09.138.
11. Acuña JJ, Jorquera MA, Barra PJ, Crowley DE, de la Luz MM. Selenobacteria selected from the rhizosphere as a potential tool for Se biofortification of wheat crops. Biol Fertil Soils. 2013;49(2):175–85. https://doi.org/10.1007/s00374-012-0705-2.
12. Xia Q, Yang Z, Shui Y, Liu X, Chen J, Khan S, Wang J, Gao Z. Methods of selenium application differentially modulate plant growth, selenium accumulation and speciation, protein, anthocyanins and concentrations of mineral elements in purple-grained wheat. Front Plant Sci. 2020. https://doi.org/10.3389/fpls.2020.01114.
13. Li L, Yu J, Li L, Rao S, Wu S, Wang S, Cheng S, Cheng H. Treatment of ginkgo biloba with exogenous sodium selenite affects its physiological growth, changes its phytohormones, and synthesizes its terpene lactones. Molecules. 2022;27(21):7548. https://doi.org/10.3390/MOLECULES27217548.
14. Li D, An Q, Wu Y, Li J-Q, Pan C. Foliar application of selenium nanoparticles on celery stimulates several nutrient component levels by regulating the α-linolenic acid pathway. ACS Sustain Chem Eng. 2020;8(28):10502–10. https://doi.org/10.1021/acssuschemeng.0c02819.
15. Domokos-Szabolcsy E, Marton L, Sztrik A, Babka B, Prokisch J, Fari M. Accumulation of red elemental selenium nanoparticles and their biological effects in *Nicotinia tabacum*. Plant Growth Regul. 2012;68:525–31. https://doi.org/10.1007/s10725-012-9735-x.
16. Cheng B, Wang C, Chen F, Yue L, Cao X, Liu X, Yao Y, Wang Z, Xing B. Multiomics understanding of improved quality in cherry radish (*Raphanus sativus* L. var. radculus pers) after foliar application of selenium nanomaterials. Sci Total Environ. 2022;824:153712. https://doi.org/10.1016/J.SCITOTENV.2022.153712.
17. El-Ramady HR, Domokos-Szabolcsy É, Abdalla NA, Alshaal TA, Shalaby TA, Sztrik A, Prokisch J, Fári M. Selenium and nano-selenium in agroecosystems. Environ Chem Lett. 2014;12:495–510. https://doi.org/10.1007/s10311-014-0476-0.
18. Li D, Zhou C, Wu Y, An Q, Zhang J, Fang Y, Li J-Q, Pan C. Nanoselenium integrates soil-pepper plant homeostasis by recruiting rhizosphere-beneficial microbiomes and allocating signaling molecule levels under Cd stress. J Hazard Mater. 2022. https://doi.org/10.1016/j.jhazmat.2022.128763.
19. Samynathan R, Venkidasamy B, Ramya K, Muthuramalingam P, Shin H, Kumari PS, Thangavel S, Sivanesan I. A recent update on the impact of nano-selenium on plant growth, metabolism, and stress tolerance. Plants. 2023;12(4):853. https://doi.org/10.3390/PLANTS12040853.
20. Rady MM, Desoky E-SM, Ahmed SM, Majrashi A, Ali EF, Arnaout SM, Selem E. Foliar nourishment with nano-selenium dioxide promotes physiology, biochemistry, antioxidant defences, and salt tolerance in *Phaseolus vulgaris*. Plants. 2021;10(6):1189. https://doi.org/10.3390/PLANTS10061189.
21. Li D, Zhou C, Ma J, Wu Y, Kang L, An Q, Zhang J, Deng K, Li J-Q, Pan C. Nanoselenium transformation and inhibition of cadmium accumulation by regulating the lignin biosynthetic pathway and plant hormone signal transduction in pepper plants. J Nanobiotechnol. 2021;19:316. https://doi.org/10.1186/S12951-021-01061-6.
22. Sa DW, Lu Q, Wang Z, Ge G, Sun L, Jia Y. The potential and effects of saline-alkali alfalfa microbiota under salt stress on the fermentation quality and microbial. BMC Microbiol. 2021;21(1):149. https://doi.org/10.1186/S12866-021-02213-2.
23. Sun P, Wang Z, Yuan N, Lu Q, Sun L, Li Y, Zhang J, Zhang Y, Ge G, Jia Y. Evaluation of nano-selenium biofortification characteristics of alfalfa (*Medicago sativa* L.). Green Process Synth. 2023;12(1):20228121. https://doi.org/10.1515/GPS-2022-8121.
24. Li Z, Wang Y, Liu J, Chen D, Feng G, Chen M, Feng Y, Zhang R, Yan X. The potential role of alfalfa polysaccharides and their sulphated derivatives in the alleviation of obesity. Food Funct. 2023. https://doi.org/10.1039/D3FO01390A.
25. Stochmal A, Piacente S, Pizza C, De Riccardis F, Leitz R, Oleszek W. Alfalfa (*Medicago sativa* L.) flavonoids. 1. Apigenin and luteolin glycosides from aerial parts. J Agric Food Chem. 2001;49(2):753–8. https://doi.org/10.1021/jf000876p.
26. Owusu-Sekyere A, Kontturi J, Hajiboland R, Rahmat S, Aliasgharzad N, Hartikainen H, Seppänen MM. Influence of selenium (Se) on carbohydrate metabolism, nodulation and growth in alfalfa (*Medicago sativa* L.). Plant Soil. 2013;373:541–52. https://doi.org/10.1007/s11104-013-1815-9.
27. Wang Q, Hu J, Hu H, Li Y, Xiang M, Wang D. Integrated eco-physiological, biochemical, and molecular biological analyses of selenium fortification mechanism in alfalfa. Planta. 2022;256(6):114. https://doi.org/10.1007/s00425-022-04027-6.
28. Zhang S, Zhu H, Cen H, Qian W, Wang Y, Ren M, Cheng Y. Effects of various forms of selenium biofortification on photosynthesis, secondary metabolites, quality, and lignin deposition in alfalfa (*Medicago sativa* L.). Field Crops Res. 2023;292:108801. https://doi.org/10.1016/J.FCR.2022.108801.
29. Wang C, Chen Z, Unteregelsbacher S, Lu H, Gschwendtner S, Gasche R, Kolar A, Schloter M, Kiese R, Butterbach-Bahl K. Climate change amplifies gross nitrogen turnover in montane grasslands of Central Europe in both summer and winter seasons. Glob Change Biol. 2016;22(9):2963–78. https://doi.org/10.1111/gcb.13353.
30. Lei H, Lian Y, Kyaw PEE, Bai M, Leghari SJ, Pan H, Xiao Z, Chen D. Using 15N isotope to evaluate the effect of brown coal application on the nitrogen fate in the soil-plant system. Agron. 2023;13(1):263. https://doi.org/10.3390/agronomy13010263.
31. Tusher VG, Tibshirani R, Chu G. Significance analysis of microarrays applied to the ionizing radiation response. PNAS. 2001;98(9):5116–21. https://doi.org/10.1073/pnas.091062498.
32. Capstaff NM, Miller AJ. Improving the yield and nutritional quality of forage crops. Front Plant Sci. 2018;9:535. https://doi.org/10.3389/fpls.2018.00535.
33. Zhu X-G, Long SP, Ort DR. Improving photosynthetic efficiency for greater yield. Annu Rev Plant Biol. 2010;61(1):235–61. https://doi.org/10.1146/annurev-arplant-042809-112206.
34. Jiang C, Zu C, Shen J, Shao F, Li T. Effects of selenium on the growth and photosynthetic characteristics of flue-cured tobacco (*Nicotiana tabacum* L.). Acta Soc Bot Pol. 2015. https://doi.org/10.5586/asbp.2015.006.
35. Golob A, Kavčič J, Stibilj V, Gaberščik A, Vogel-Mikuš K, Germ M. The effect of selenium and UV radiation on leaf traits and biomass production in *Triticum aestivum* L. Ecotoxicol Environ Saf. 2017;136:142–9. https://doi.org/10.1016/j.ecoenv.2016.11.007.
36. Qiu Z, Wang L, Zhou Q. Effects of bisphenol A on growth, photosynthesis and chlorophyll fluorescence in above-ground organs of soybean seedlings. Chemosphere. 2013;90(3):1274–80. https://doi.org/10.1016/j.chemosphere.2012.09.085.
37. Zhang M, Tang S, Huang X, Zhang F, Pang Y, Huang Q, Yi Q. Selenium uptake, dynamic changes in selenium content and its influence on photosynthesis and chlorophyll fluorescence in rice (*Oryza sativa* L.). Environ Exp Bot. 2014;107:39–45. https://doi.org/10.1016/j.envexpbot.2014.05.005.

38. Kirst H, Gabilly ST, Niyogi KK, Lemaux PG, Melis A. Photosynthetic antenna engineering to improve crop yields. Planta. 2017;245:1009–20. https://doi.org/10.1007/s00425-017-2659-y.
39. El-Ramady H, Abdalla N, Taha HS, Alshaal T, El-Henawy A, Faizy SE-DA, Shams MS, Youssef SM, Shalaby T, Bayoumi Y. Selenium and nano-selenium in plant nutrition. Environ Chem Lett. 2016;14:123–47. https://doi.org/10.1007/s10311-015-0535-1.
40. Ning C, Ding N, Wu G, Meng H, Wang Y, Wang Q. Proteomics research on the effects of applying selenium to apple leaves on photosynthesis. Plant Physiol Biochem. 2013;70:1–6. https://doi.org/10.1016/j.plaphy.2013.05.008.
41. Sors TG, Ellis DR, Salt DE. Selenium uptake, translocation, assimilation and metabolic fate in plants. Photosynth Res. 2005;86:373–89. https://doi.org/10.1007/s11120-005-5222-9.
42. Valle G, McDowell L, Prichard D, Chenoweth P, Wright D, Martin F, Kunkle W, Wilkinson N. Selenium concentration of fescue and bahiagrasses after applying a selenium fertilizer. Commun Soil Sci Plant Anal. 2002;33(9–10):1461–72. https://doi.org/10.1081/CSS-120004294.
43. Gupta M, Gupta S. An overview of selenium uptake, metabolism, and toxicity in plants. Front Plant Sci. 2017. https://doi.org/10.3389/fpls.2016.02074.
44. Leghari SJ, Wahocho NA, Laghari GM, HafeezLaghari A, MustafaBhabhan G, HussainTalpur K, Bhutto TA, Wahocho SA, Lashari AA. Role of nitrogen for plant growth and development: a review. Adv Environ Biol. 2016;10(9):209–19.
45. Coruzzi G, Bush DR. Nitrogen and carbon nutrient and metabolite signaling in plants. Plant Physiol. 2001;125(1):61–4. https://doi.org/10.1104/pp.125.1.61.
46. Sun Y, Wang M, Mur LAJ, Shen Q, Guo S. Unravelling the roles of nitrogen nutrition in plant disease defences. Int J Mol Sci. 2020;21(2):572. https://doi.org/10.3390/ijms21020572.
47. Pate J. Uptake, assimilation and transport of nitrogen compounds by plants. Soil Biol Biochem. 1973;5(1):109–19. https://doi.org/10.1016/0038-0717(73)90097-7.
48. Dyckmans J, Scrimgeour CM, Schmidt O. A simple and rapid method for labelling earthworms with ^{15}N and ^{13}C. Soil Biol Biochem. 2005;37(5):989–93. https://doi.org/10.1016/j.soilbio.2004.10.017.
49. Chalk PM, Peoples MB, McNeill AM, Boddey RM, Unkovich MJ, Gardener MJ, Silva CF, Chen D. Methodologies for estimating nitrogen transfer between legumes and companion species in agro-ecosystems: a review of ^{15}N-enriched techniques. Soil Biol Biochem. 2014;73:10–21. https://doi.org/10.1016/j.soilbio.2014.02.005.
50. Garnett T, Conn V, Kaiser BN. Root based approaches to improving nitrogen use efficiency in plants. Plant, Cell Environ. 2009;32(9):1272–83. https://doi.org/10.1111/j.1365-3040.2009.02011.x.
51. Campbell WH. Nitrate reductase structure, function and regulation: bridging the gap between biochemistry and physiology. Annu Rev Plant Biol. 1999;50(1):277–303. https://doi.org/10.1146/annurev.arplant.50.1.277.
52. Einsle O, Messerschmidt A, Stach P, Bourenkov GP, Bartunik HD, Huber R, Kroneck PM. Structure of cytochrome c nitrite reductase. Nature. 1999;400(6743):476–80. https://doi.org/10.1038/22802.
53. Rossato L, Lainé P, Ourry A. Nitrogen storage and remobilization in *Brassica napus* L. during the growth cycle: nitrogen fluxes within the plant and changes in soluble protein patterns. J Exp Botany. 2001;52(361):1655–63. https://doi.org/10.1093/jexbot/52.361.1655.
54. Feller U, Fischer A. Nitrogen metabolism in senescing leaves. Crit Rev Plant Sci. 2011;13(3):241–73. https://doi.org/10.1080/07352689409701916.
55. Li D, Zhou C, Zou N, Wu Y, Zhang J, An Q, Li J-Q, Pan C. Nanoselenium foliar application enhances biosynthesis of tea leaves in metabolic cycles and associated responsive pathways. Environ Pollut. 2021;273:116503. https://doi.org/10.1016/J.ENVPOL.2021.116503.
56. Zhu Z, Zhang Y, Liu J, Chen Y, Zhang X. Exploring the effects of selenium treatment on the nutritional quality of tomato fruit. Food Chem. 2018;252:9–15. https://doi.org/10.1016/j.foodchem.2018.01.064.
57. Wu X, Liu Y, Yin S, Xiao K, Xiong Q, Bian S, Liang S, Hou H, Hu J, Yang J. Metabolomics revealing the response of rice (*Oryza sativa* L.) exposed to polystyrene microplastics. Environ Pollut. 2020;266:115159. https://doi.org/10.1016/j.envpol.2020.115159.
58. Lee HS, Hwang WH, Jeong JH, Ahn SH, Baek JS, Jeong HY, Park HK, Ku BI, Yun JT, Lee GH. Analysis of the distribution of assimilation products and the characteristics of transcriptomes in rice by submergence during the ripening stage. BMC Genomics. 2019;20:1–16. https://doi.org/10.1186/s12864-018-5320-7.
59. Maleki S, Mærk M, Valla S, Ertesvåg H. Mutational analyses of glucose dehydrogenase and glucose-6-phosphate dehydrogenase genes in *Pseudomonas fluorescens* reveal their effects on growth and alginate production. Appl Environ Microbiol. 2015;81(10):3349–56. https://doi.org/10.1128/AEM.03653-14.
60. Zhang Z, TeSlaa T, Xu X, Zeng X, Yang L, Xing G, Tesz GJ, Clasquin MF, Rabinowitz JD. Serine catabolism generates liver NADPH and supports hepatic lipogenesis. Nat Metab. 2021;3(12):1608–20. https://doi.org/10.1038/S42255-021-00487-4.
61. Xu J-Z, Yang H-K, Zhang W-G. NADPH metabolism: a survey of its theoretical characteristics and manipulation strategies in amino acid biosynthesis. Crit Rev Biotechnol. 2018;38(7):1061–76. https://doi.org/10.1080/07388551.2018.1437387.
62. Tang N, Huang W, Li X, Gao X, Liu X, Wang L, Xing W. Drilling into the physiology, transcriptomics, and metabolomics to enhance insight on *Vallisneria denseserrulata* responses to nanoplastics and metalloid co-stress. J Cleaner Prod. 2024;448:141653. https://doi.org/10.1016/J.JCLEPRO.2024.141653.
63. Liu C, Zhou G, Qin H, Guan Y, Wang T, Ni W, Xie H, Xing Y, Tian G, Lyu M. Metabolomics combined with physiology and transcriptomics reveal key metabolic pathway responses in apple plants exposure to different selenium concentrations. J Hazard Mater. 2024;464:132953. https://doi.org/10.1016/J.JHAZMAT.2023.132953.
64. Ferrer J, Austin M, Stewart C Jr, Noel J. Structure and function of enzymes involved in the biosynthesis of phenylpropanoids. Plant Physiol Biochem. 2008;46(3):356–70. https://doi.org/10.1016/j.plaphy.2007.12.009.
65. Abdel-Lateif K, Vaissayre V, Gherbi H, Verries C, Meudec E, Perrine-Walker F, Cheynier V, Svistoonoff S, Franche C, Bogusz D. Silencing of the chalcone synthase gene in C asuarina glauca highlights the important role of flavonoids during nodulation. New Phytol. 2013;199(4):1012–21. https://doi.org/10.1111/nph.12326.
66. Gąsecka M, Mleczek M, Siwulski M, Niedzielski P, Kozak L. The effect of selenium on phenolics and flavonoids in selected edible white rot fungi. LWT-Food Sci Technol. 2015;63(1):726–31. https://doi.org/10.1016/j.lwt.2015.03.046.
67. Rao S, Gou Y, Yu T, Cong X, Gui J, Zhu Z, Zhang W, Liao Y, Ye J, Cheng S. Effects of selenate on Se, flavonoid, and glucosinolate in broccoli florets by combined transcriptome and metabolome analyses. Food Res Int. 2021;146:110463. https://doi.org/10.1016/J.FOODRES.2021.110463.
68. König S, Feussner K, Kaever A, Landesfeind M, Thurow C, Karlovsky P, Gatz C, Polle A, Feussner I. Soluble phenylpropanoids are involved in the defense response of A rabidopsis against V erticillium longisporum. New Phytol. 2014;202(3):823–37. https://doi.org/10.1111/nph.12709.
69. Mo Y, Nagel C, Taylor LP. Biochemical complementation of chalcone synthase mutants defines a role for flavonols in functional pollen. PNAS. 1992;89(15):7213–7. https://doi.org/10.1073/pnas.89.15.7213.
70. Rencoret J, Rosado MJ, Kim H, Timokhin VI, Gutiérrez A, Bausch F, Rosenau T, Potthast A, Ralph J, Del Río JC. Flavonoids naringenin chalcone, naringenin, dihydrotricin, and tricin are lignin monomers in papyrus. Plant Physiol. 2022;188(1):208–19. https://doi.org/10.1093/PLPHYS/KIAB469.
71. Mahon EL, de Vries L, Jang S-K, Middar S, Kim H, Unda F, Ralph J, Mansfield SD. Exogenous chalcone synthase expression in developing poplar xylem incorporates naringenin into lignins. Plant Physiol. 2022;188(2):984–96. https://doi.org/10.1093/plphys/kiab499.

Publisher's Note

Springer Nature remains neutral with regard to jurisdictional claims in published maps and institutional affiliations.